Extraction modeling, kinetics and thermodynamics of solvent extraction of *Irvingia gabonensis* kernel oil, for possible industrial application

[1]**Chinedu Matthew Agu*** [1]**Matthew Chukwudi Menkiti** [1]**Paschal Enyinnaya Ohale** [1]**Victor Ifeanyi Ugonabo**

[1] **Chemical Engineering Department, Nnamdi Azikiwe University, Awka, Nigeria.**

*Corresponding author: eduetal@yahoo.com

Abstract

Temperature, time and particle size effects on *Irvingia gabonensis* kernel oil (IGKO) yield, as well as the kinetics and thermodynamics parameters were investigated. Highest oil yield of 68.80 % (by weight) was obtained at 55 °C, 150 min., and 0.5 mm. Evaluated physicochemical properties of IGKO indicated that viscosity, acidity, dielectric strength, flash and pour points were 19.37 mm^2s^{-1}, 5.18 mg $KOHg^{-1}$, 25.83 KV, 285 °C, and 17 °C, respectively, suggesting its feasibility as transformer fluid upon further treatment. Of the pseudo second order (PSO) and hyperbolic kinetic models studied, the former gave better fit to the experimental data. ΔH, ΔS and ΔG values of IGKO extraction at 0.5 mm and 328 K were, 251.81 KJ/mol, 1.08 KJ/mol and -105.49 KJ/mol, respectively, indicating the endothermic, irreversible and spontaneous nature of the process. Kinetic model equations that describe the process were successfully developed for both models based on the process parameters.

Keywords: Solvent extraction; *Irvingia gabonensis*; Kinetics; Thermodynamics; modeling

1. Introduction

The searches for suitable alternative to petroleum have increased in recent years. This is attributed to human-induced global climate change, depleted petroleum reserve and more recently the drop in the global crude oil price. In Nigeria, prior to the commencement of crude oil exploration and production in February 1958 by Shell British Petroleum at Oloibiri and Afam oil fields in Port Harcourt; agriculture was the main stay of the economy [1-2]. As a result of these, especially the drop in the global crude oil, Nigerian government have introduced measures and polices that are geared towards the diversification of the economy, with special attention given to agricultural development. This government initiative has led to the development of the agricultural sectors that is aimed at achieving food security, industrial utilization of its products, job creation, as well as products processing for export purposes.

32   The aftermath of this is the massive planting of economic trees, oil seeds and nuts etc. [3] that

33   could serve as source of biodegradable oil for petroleum substitution. Some of such oil seeds

34   and nuts include but not limited to *Irvingia gabonensis* (IG), soya bean, palm trees, *Jatropha*

35   *curcas*, groundnut, *Terminalia catappa* L etc.

36   *Irvingia gabonensis* otherwise known as wild bush mango or "Ogbono" in south eastern part

37   of Nigeria is a member of the Simarubaceae family [4]. It is an economic tree with its origin

38   traced to most tropical forest of West and Central Africa [5]. In West Africa, *Irvingia*

39   *gabonensis* is seen as the most important tree being encouraged for domestication [6-7].

40   Thus, it has attracted the attention of the World Agroforestry Centre (formerly the

41   International Centre for Research in Agroforestry, ICRAF), together with its partners, thereby

42   making it their choice tree in their agroforestry tree domestication programme [7-8].

43   Seasonally (between April to July), *Irvingia gabonensis* tree produces lots of edible fruits

44   with limited consumption of the fresh fruits [5]. However, there is greater utilization of the

45   kernel. As a result of this, it is a common practice to split the fruit into two using cutlass, in

46   other to remove the split cotyledon (kernel) with knife. Thereafter, the flashy mesocarp is

47   discarded to rot, while the kernel is used for number of purposes [9].

48   Over the years, researches on *Irvingia gabonensis* kernel (IGK) have mainly been on its

49   nutritional and medicinal applications, as well as the used of the milled kernels as condiment

50   in soup as thickener, due to its rich fat and protein content [10-12]. Medicinally, it is used in

51   body weight reduction of obese persons [13], with little attention to its industrial applications.

52   However, its kernels have been found to have local industrial application, as it is used in the

53   making of local soap, due its high oil content [14]. Previously, researches have shown that

54   IGK exhibits very high oil content which ranges between 60% and 69.76%. Hence, makes

55   it's industrially utilization very attractive [11, 15-17]. Never the less, few researches have

56   been conducted on the possible application of *Irvingia gabonensis* kernels oil (IGKO)

57 industrially for biodiesel production [15]. Therefore, there is need to extend the utilization of

58 IGKO in the production of transformer oil (TO), since to the best knowledge of the authors, no

59 published work have been recorded in this direction [18].

60 Prior to the use of vegetable oil like IGKO for industrial applications, there is need for the oil

61 to be extracted from the seeds/kernels. In other to achieve this goal, the choice of extraction

62 method becomes very important [19]. Several extraction methods exist. Some of these

63 methods are solvent extraction, sonication-assisted extraction; microwave-assisted extraction,

64 supercritical fluid extraction, accelerated solvent extraction etc [20]. However, solvent

65 extraction method using soxhlet extractor was adopted in this study because of its simplicity,

66 high oil yield and oil quality associated with the method [20-21]. Solvent extraction method

67 has been utilized severally for extraction of oil from fruits, seeds and nuts. Some of such fruits,

68 seeds and nuts include Hazelnut (*Corylus avellana L.*) [22], *Maclura pomifera* (Rafin.)

69 Schneider seed [23], *Prunus armeniaca L*. [24], Sacha inchi (*Plukenetia volubilis*) seeds [25],

70 coconut waste [26]. Similarly, *Irvingia gabonensis* is not left out, as solvent extraction

71 methods have been utilized to extract oil from it [11,15]. It is important to state that in solvent

72 extraction, the knowledge of the kinetic of oil extraction is of paramount importance. This is

73 because it assists in the determination of the highest oil yield within the studied time intervals

74 [27]. In other words, the need carry out extensive study on the kinetics of oil extraction from

75 *Irvingia gabonensis* seed kernels.

76 Previously, researchers have carried out studies on the kinetics of oil extraction from seeds,

77 and nuts. For instance, oil extraction kinetics have been applied to the extraction of oil from

78 *Jatropha curcas* [28], sunflower seeds [29-30], fluted pumpkin seed [31], coconut waste [26],

79 Neem seed (*Azadirachta indica A. Juss*) [32] and *Prunus persica* [33]. It is therefore very

80 necessary to study the kinetics of oil extraction process of different varieties of seed or nut.

81 This is because from literature, it has been established that the ease of extraction of oil from

82 seed/nuts varies [34]. Therefore, the study of the kinetics of oil extraction from *Irvingia*

83 *gabonensis* kernels becomes very important, since to the best of knowledge of the authors,

84 there haven't been any published work in that regard.

85 It is worth knowing that during oil extraction process, the extraction rate (the rate at which

86 equilibrium is attained) is influenced by factors like, solute and solvent diffusion capacity,

87 size, shape, internal structure of seeds particles (matrix), and the dissolution rate of the

88 solvent on the oil soluble substances (solute) [21]. In other words, the kinetics of *Irvingia*

89 *gabonensis* kernel oil (IGKO) extraction consists of the releasing of oil from porous or

90 cellular matrices, into the solvent through the process of mass transfer mechanisms. This oil

91 (solute) linked to the solid matrix of the kernel particles by either physical or chemical forces

92 must be transported to the solvent phase by dissolution process [35]. For this to occur, three

93 important steps have to be taken into consideration: (1) solvent penetration into the seed

94 matrix (tissue), (2) intercellular miscella formation, and (3) extracted oil diffusion into the

95 exterior miscella [27]. In other words, mathematical modeling of oil extraction kinetics from

96 seeds and nuts is an activity of great importance. This is due to its economic benefits to

97 industries. In the light of this and other benefits, it is necessary to develop models for

98 extraction process based on the process parameters. In order to achieve this, the estimated

99 process parameters, needs to be used in the development of the model that considers the

100 phase behavior, state of equilibrium, solubility, diffusion and dissolution of the process [35-

101 36]. Several models have been used by researchers in the study of oil extraction kinetics

102 process for oil seeds like, olive cake [37], sunflower [38-39], rapeseed (canola) [27].

103 However, while extraction kinetics has been extensively studied by many researchers, there is

104 limited or no studies in the literature on that of oil extraction kinetics and thermodynamics of

105 *Irvingia gabonensis* kernels oil extraction. Therefore, the objectives of this study were to

106 study the influence of process parameters of temperature, time, and particle size on IGK oil

yield, as well as to fit the obtained experimental data into two closely related extraction kinetic

models (hyperbolic and pseudo second order), so as to determine the model that best fit the

experimental kinetic data. Also, the kinetic models of the extraction processes under different

process parameters were established for predicting the extraction processes. Additionally, the

coefficient of determination (R^2) and for statistical error analysis functions [root mean square

(RMS), the average relative error (ARE%) and the standard error of estimation (SEE)], were

used to study the fitting of the extraction kinetics models to the experimentally obtained

kinetics data. Furthermore, Arrhenius equation was used to evaluate the effect of extraction

temperature on the kinetic models. The thermodynamic parameters of oil extraction from

Irvingia gabonensis kernels were also evaluated. Furthermore, the physicochemical

characterization of the IGKO was carried with the aim of evaluating its potentiality as base

fluid for transformer oil production. Finally, Fourier Transform Infrared (FTIR) was

afterwards used to ascertain the functional groups present in the IGKO.

2. Materials and methods

2.1. Sample collection and preparation

Irvingia gabonensis kernels (IGK) were procured from Nkwo-Agu market, Umuaga in Udi

Local Government Area, Enugu State, Nigeria. They were oven dried at temperature of 60 °C

for 12 h. Thereafter, the dried samples were milled using manual grinder. They were then

sieved with different sieve sizes to obtain five different average particle sizes (0.5, 1.0, 1.5,

2.0 and 2.5 mm). The ground samples were sealed and stored until they were ready for use.

2.2. Solvent extraction experiment using Soxhlet extractor

15 g of dried milled IGK powder of a particular particle size was packed in a thimble of the

soxhlet extractor. The extractor was then filled with 150 ml of n-hexane. The experiments

were performed at five different temperatures (35, 40, 45, 50, and 55 °C) and at five different

extraction times (30, 60, 90, 120, and 150 min) for each particular average particle size (0.5,

1.0, 1.5, 2.0 and 2.5 mm). The extraction temperature was measured using an electronic thermometer (± 0.1°C, Hanna HI-9063), while the time was measured using a stop watch. The oil yield was calculated using AOAC method no. 920.85 [40] using automatic soxhlet apparatus (Soxtec 2050 FOSS, Denmark) in line with manufacturer manual guidelines. After each extraction process, the solvent was removed at 60 °C using rotary evaporator (model N-1000S-W, EYELA, Tokyo, Japan). The extraction done under every set of conditions was performed three times and the average value recorded. The oil yield of IGK was calculated using equation (1).

$$\% \, Yield \, = \, \frac{weight \, of \, oil \, extracted \, (g)}{weight \, of \, sample \, (g)} \times 100 \, \%$$ (1)

2.3. Kinetics

The analysis and design of extraction processes needs relevant kinetic data since it is the most important information to be used to understand the extraction process. In order to obtain these kinetic data, experiments were carried out at temperatures (35, 40, 45, 50, and 55 °C) and at extraction times (30, 60, 90, 120, and 150 min) for each particular particle size (0.5, 1.0, 1.5, 2.0 and 2.5 mm) as stated earlier. Thereafter, the obtained experimental kinetics data were fitted to hyperbolic and pseudo second order models.

2.3.1. Hyperbolic model

Hyperbolic model has been applied in food engineering science as peleg's model in equation (2).

$$c \, = \, c_0 \, + \, \frac{t}{K_1 + K_2 t}$$ (2)

Where K_1 is the model rate constant, K_2 is the model capacity constant, c is the concentration of solute in the extraction solvent at any time (g L^{-1}) and c_0 is the initial concentration of the solute in the sample particle (g m^{-3}) and is usually equal to zero.

155 Therefore, the extraction curves (% oil yield vs. time) exhibits similar sharp as the sorption

156 curves (moisture content vs. time) proposed by peleg. Hence, the feasibility of using the same

157 mathematical model proposed by peleg [41] to describe the kinetics of oil extraction from

158 *Irvingia gabonensis* kernels.

159 However, in this case, the extraction rate at the very beginning C_1 (min^{-1}) and constant related

160 to maximum extraction yield C_2 (min^{-1}) were taken into consideration [19]. Thus, the

161 hyperbolic model used to describe the oil extraction from *Irvingia gabonensis* kernels is

162 expressed as in equation (3).

163 $\bar{y} = \dfrac{C_1 t}{1 + C_2 t}$ (3)

164 Recently, equation (3) has been used to model the extraction of resinoid from aerial parts of

165 St. John's wort (*Hypericum perforatum L.*) [19], extraction of protopine from *Fumaria*

166 *officinalis L.* [42], as well as in the extraction of total polyphenols from grapes [43]. Equation

167 (3) results from a second order rate law as could be seen in equation (4). As such, it is

168 important to state that peleg's model [41] and pseudo second-order integrated rate law,

169 equation (4), are both hyperbolic equations [44].

170 $C_t = \dfrac{C_t^2 kt}{1 + C_s kt}$ (4)

171 Where $C_t^2 k$ and $C_s k$ in equation (4) are equivalent to C_1 and C_2 respectively in equation (3). k

172 is the second order extraction rate constant while C_t and C_s are the concentrations of oil in the

173 solution at any time t and at saturation, respectively (g L^{-1}).

174 From equation (3), it is important to state that the extraction is first-order at the very onset, and

175 drops to zero-order in the latter phase of the extraction process. As such, when $C_2 t \ll 1$,

176 equation (3) reduces to equation (5).

177     $\bar{y} \approx C_1 t$ (5)

178   And when t → s, the equilibrium is reached($y_i = y_e$), so

179     $\bar{y}_e = \frac{y_e}{y_0} = \frac{C_1}{C_2}$ (6)

180   Hence, C_1 is a constant that is related to the rate of extraction at the beginning, while the ratio

181   C_1/C_2, the peleg capacity constant which is related to the maximum of extraction yield, is the

182   equilibrium concentration of the extracted oil.

183   When equation (3) is linearized, equation (7) is obtained.

184     $\frac{1}{\bar{y}} = \frac{1}{C_1} \times \frac{1}{t} + \frac{C_2}{C_1}$ (7)

185   The plot of $1/\bar{y}$ (that is 1/yield) against 1/t, gives intercept as C_2/C_1 and slope as $1/C_1$.

186   **2.3.2. Pseudo second-order model**

187   The second-order rate law had been used over the years to model solvent extraction of a

188   number of substances from plants, leaves, seeds and nuts [45-46]. Extraction kinetic models

189   that are based on a second-order rate law are usually used in both conventional and non-

190   conventional extractions [45-46]. It provides a suitable illustration of solid-liquid extraction

191   process as such it was applied to describe the kinetics of oil extraction from *Irvingia*

192   *gabonensis* kernels.

193   For a second-order rate law, the rate of dissolution of the oil contained in the solid to solution

194   can be described by equation (8).

195     $\frac{dC_t}{dt} = k\,(C_s - C_t)^2$ (8)

196   Where:

197     $\frac{dC_s}{dt} = the\ extraction\ rate\ (g\ L^{-1}\ min^{-1})$

198   k = the second-order extraction rate constant (L g^{-1}min^{-1})

199   C_s = the extraction capacity (concentration of oil at saturation in g L^{-1})

200    $C_t = \bar{y}$ = the concentration of oil in the solution at any time (g L^{-1}), t (min)

201   By taking the initial and boundary condition t = 0 to t = t and C_t = 0 to C_t=C_t, the integrated

202   rate law for pseudo second-order extraction was obtained as equation (9).

203    $$C_t = \frac{C_t^2 kt}{1 + C_s kt} \tag{9}$$

204   The linearized form of equation (9) is equation (10).

205    $$\frac{C_t}{t} = \frac{1}{(1/KC_s^2)(t/C_s)} \tag{10}$$

206   This can be further linearized in the form of equation (11).

207    $$\frac{t}{C_t} = \frac{1}{KC_s^2} + \frac{t}{C_s} \tag{11}$$

208   Thus, as t approaches 0, the initial extraction rate, h, is written as in equation (12).

209    $$h = KC_s^2 \tag{12}$$

210   When equation (10) is rearranged, the concentration of oil at any time can be obtained,

211   equation (13).

212    $$C_t = \frac{t}{\frac{1}{h} + \frac{t}{C_s}} \tag{13}$$

213   The initial extraction rate, h, the extraction capacity, C_s and the pseudo second order

214   extraction, k, can be calculated experimentally by plotting t/C_t vs t where by C_s and k are

215   determined from the intercept and slope of the linear plot, respectively.

2.4. Temperature effects

217   Arrhenius equation was used in evaluating the effect of temperature of extraction on the

218   kinetic models. That is, it was used to describe the relationship between extraction rate

219   constant (k) and temperature (T). Equation (14) shows the Arrhenius equation.

220　$Ln\ k\ =\ Ln\ k_0\ +\ \left(-\ \dfrac{E_a}{R}\ \times\ \dfrac{1}{T}\right)$ (14)

221　Rearranging the above equation (14), results to equation (15).

222　$k\ =\ k_0 e^{\frac{-E_a}{RT}}$ (15)

223　Equation (15) can also be re-written in the form shown in equation (16). When this is done,

224　the unit of E_a is written as (KJ mol^{-1}).

225　$k\ =\ k_0 exp\left(-\ \dfrac{1000 E_a}{RT}\right)$ (16)

226　Where k_0 is the pre-exponential factor for extraction rate constant (Lg^{-1} min^{-1}), E_a represents

227　the activation energy of extraction (J mol^{-1}). R is the ideal gas constant (8.314 J mol^{-1} K^{-1}), T

228　is the temperature of extraction (K). The pre-exponential factor, k_0 and the activation energy,

229　E_a can be determined using the natural logarithm of Eq. (15). The plot of Ln (k) against

230　1000/T was used to calculate k_0 and E_a.

231　**2.5. Thermodynamic parameters**

232　The thermodynamic parameters enthalpy change (ΔH) and entropy change (ΔS), for the

233　extraction of oil from *Irvingia gabonensis* kernels were calculated using Van't Hoff equation

234　(17).

235　$Ln\ K\ =\ -\ \dfrac{\Delta H}{RT}\ +\ \dfrac{\Delta S}{R}$ (17)

236　Equation (17) can be re-written to include the Gibbs free energy change in the form of

237　equation (18).

238　$Ln\ K\ =\ \dfrac{\Delta G}{RT}\ =\ -\ \dfrac{\Delta H}{RT}\ +\ \dfrac{\Delta S}{R}$ (18)

239　The Gibbs free energy change was calculated using equation (19).

240     $\Delta G = \Delta H - T \cdot \Delta S$ (19)

241     $K = \dfrac{Y_T}{Y_u} = \dfrac{m_L}{m_S}$ (20)

242   Where K is equilibrium constant, Y_T is the yield of oil at temperature T, Y_u is the percentage

243   of the un-extracted oil, m_L is amount of IGK in liquid at equilibrium temperature T, m_s is

244   amount of IGK in solid at equilibrium temperature T, R is gas constant (8.314J/mol K), while

245   ΔH (kJ/mol), ΔS (kJ/mol), and ΔG (kJ/mol) are enthalpy, entropy and Gibbs free energy,

246   respectively.

247   **2.6. Statistical Analysis**

248   The degree at which the models studied statistically represent the data obtained

249   experimentally were by the evaluation of correlation coefficient (R^2) using equation (21), the

250   root mean square (RMS) [19], the average relative error (ARE%) [47] and the standard error

251   of estimation (SEE) [47]. The error functions were computed using the expressions in

252   equations (22), (23) and (24) for RMS, ARE and SEE, respectively.

253     $R^2 = \dfrac{\sum_{N=1}^{N}\left(\bar{y}_{exp} - \bar{y}_{cal}\right)^2}{\sum_{N=1}^{N}\left(\bar{y}_{exp} - \bar{y}_{cal}\right)^2}$ (21)

254     $RMS = \sqrt{\dfrac{1}{N}\sum_{i=1}^{N}\left(\dfrac{\bar{y}_{exp} - \bar{y}_{cal}}{\bar{y}_{exp}}\right)^2}$ (22)

255     $ARE = \dfrac{100}{N} \times \sum \dfrac{|x - y|}{x}$ (23)

256     $SEE = \sqrt{\dfrac{\sum(x - y)^2}{dt}}$ (24)

257 Where N is the number of experimental data points. $\overline{y}_{cal}$ and $\overline{y}_{exp}$ are the calculated and

258 experimental values, respectively, in equations 22. Similarly, x and y are experimental and

259 calculated values, respectively in equations 23 and 24.

2.7. Physicochemical properties of *Irvingia gabonensis* kernels oil (IGKO)

261 IGKO was characterized after it was extracted. The oil density (AOAC 985.19), iodine value

262 (AOAC 993.20) and acid value (AOAC 969.17), were determined according to AOAC

263 official technique [48]. On the other hand, the viscosity and dielectric strength were measured

264 according to ASTM D445, [49] and IEC 60156, [50] standard methods, respectively. The oil

265 samples were tested three times and the average value taken.

2.8. Fourier transform infrared spectroscopy (FTIR) analysis

267 The FTIR analysis of the IG oil sample was carried out using BUCK Scientific Infrared

268 Spectrophotometer Model 530.

3. Results and discussion

3.1. Experimental results

3.1.1. Effect of temperature

272 Temperature of extraction is one of the most essential parameter in extraction process. This is

273 because of the very high sensitivity of the chemical constituent of plants, seeds, nuts, kernels

274 and leaves to heat. Solute solubility, as well as the diffusion coefficient, increases with the

275 increase in the extraction temperature, as such, influencing the extraction process [51].

276 The effect of temperature on extraction rate of oil from IGK has been studied over

277 temperatures range of 35 – 55 °C, keeping the particle size constant at particle sizes (0.5, 1.0,

278 1.5, 2.0 and 2.5 mm), in each case [Fig. 1 (a – e)]. It could be observed that increase in

279 temperature from 35 to 55 °C, resulted in the increase of the oil extraction yield irrespective

280 of the solute particle size. This could be attributed to the increase in diffusion of oil with

281   decrease in its viscosity as the temperatures increased [26,52]. Similarly, the mass transfer

282   coefficient of the process also increased with temperature thereby affecting diffusion [26].

283   Fig. 1(a – e) shows the extraction of oil from IGK using soxhlet extractor operated at

284   maximum time of 150 mins. It could be seen that the rate of extraction was fast at the

285   beginning of the process, and gradually reduces. This was due to the dissolution of free oil

286   from the surface of the IGK when exposed to the fresh solvent, thereby leading to quick oil

287   extraction. This leads to fast increase in the rate of extraction. This was in agreement with the

288   findings of Sulaiman et al. [26] and Sayyar et al. [53] for the extraction of solid coconut

289   waste and jatropha seeds oils, respectively.

290

291

292

293

294

295

296
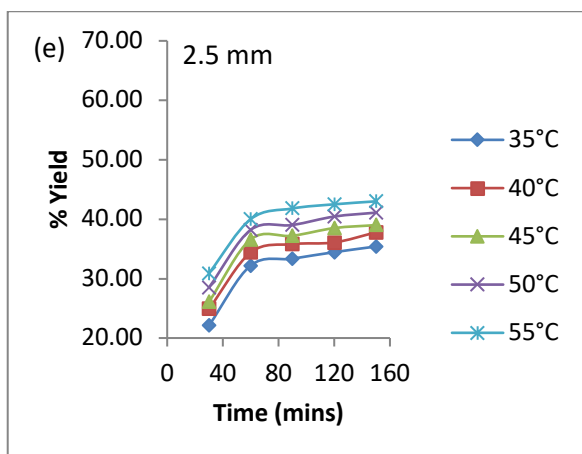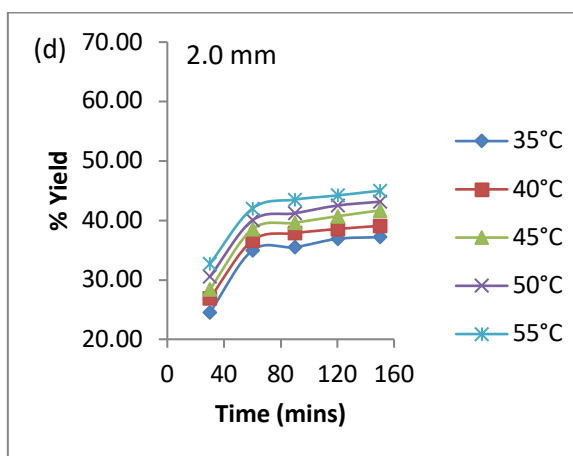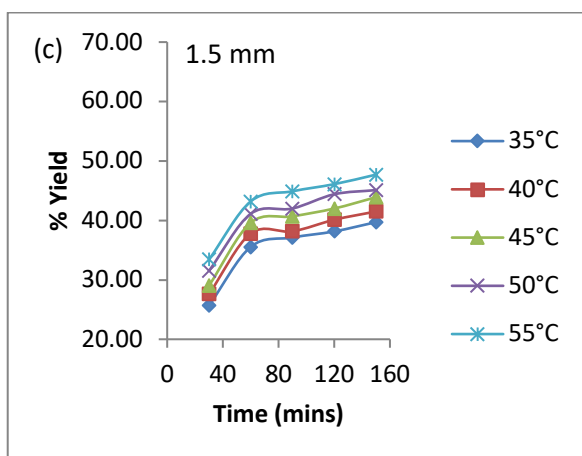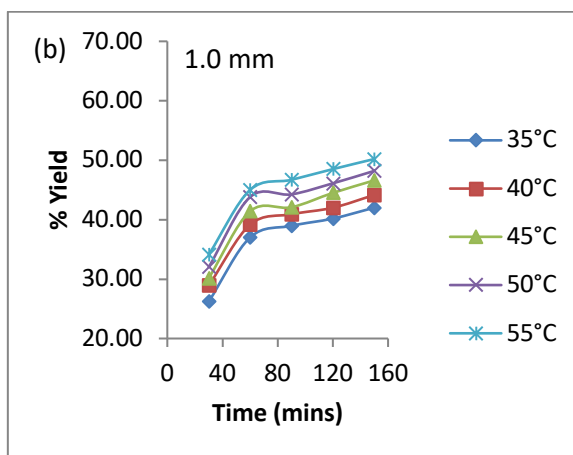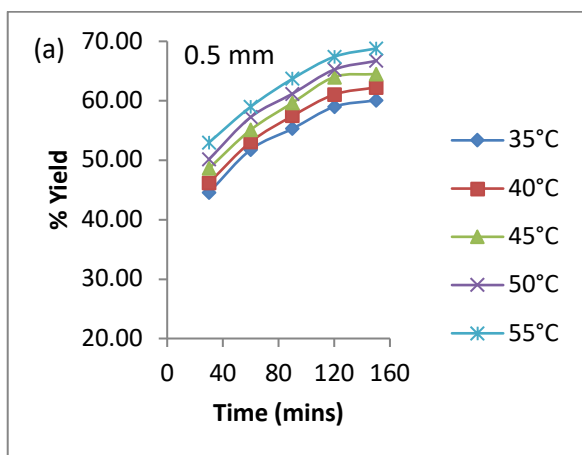
Fig. 1: Effect of temperature on the oil yield of IGK at different average particle sizes (mm): (a) 0.5, (b) 1.0, (c) 1.5, (d) 2.0, and (e) 2.5 mm

3.1.2. Effect of particle size

Extraction rate increases as the particle size decreases [26,54]. Fig. 2a and b shows the effect of particle size on the extraction of oil from IGK using hexane as solvent. The particle sizes

308 considered in this study were 0.5, 1.0, 1.5, 2.0 and 2.5 mm. It could be seen that their

309 (particles sizes) respective oil yields were 60.08, 42.01, 39.70, 37.18 and 35.4 %, at 35 °C

310 and 150 mins. This shows that highest oil yield was obtained with the smallest particle size of

311 0.5 mm, and the least with the largest particle size of 2.5 mm. These findings were in line

312 with the works of Sulaiman et al. [26] and Huang et al. [55], for the extractions of solid

313 coconut waste oil and Baizhu, respectively.

314 The additional oil extracted from smaller particle size was attributed to the larger interfacial

315 area of the solid present in them. Also, the solvent requires minimal distance to penetrate the

316 solid particles in other to extract oil from it. In other words, contributes to increase in pore

317 diffusion between the solute (solid) and the solvent. On the other hand, larger particles have

318 limited contact surface area, which causes more resistance to solvent penetration and oil

319 diffusion. Hence, smaller quantity of oil would be transported from the inside of the larger

320 particles to the surrounding solution [26,53].
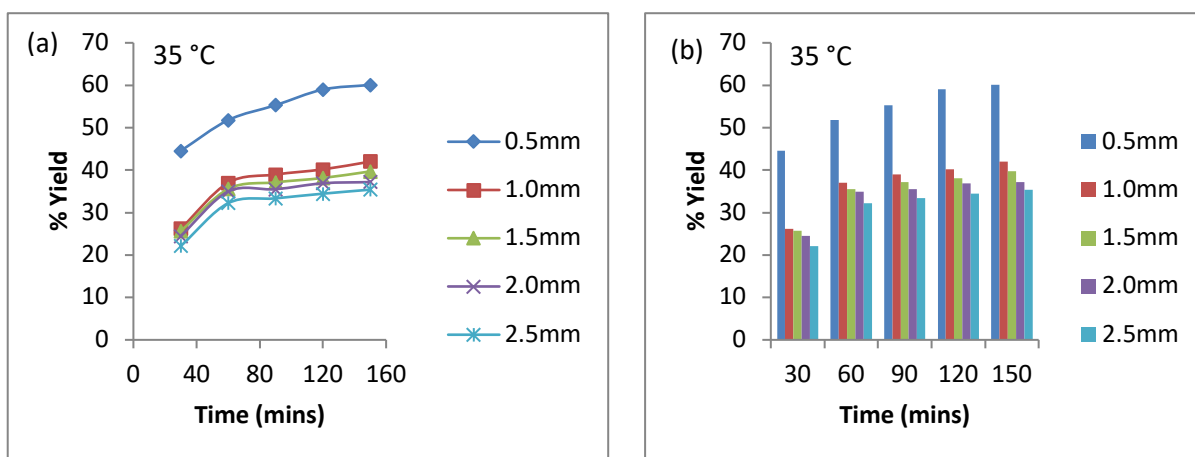
321
322 **Fig. 2: Effect of particle size on percentage oil yield of IGK at 35 °C**

323

324 **3.2. Kinetic parameters**

325 The values of the kinetic parameters and the individual error estimates for the nonlinear

326 kinetics of hyperbolic and pseudo second order models are presented in Table 1. In Table 1, it

327 could be observed that majority of the kinetic parameters of C_1 and C_s for hyperbolic and

328   Pseudo second order models, respectively, increased with the increase in temperature. This

329   could be attributed to the reason behind the increase in the oil yield as temperature increased

330   [18,42]. Similarly, the kinetic parameters of C_2 and K also increased with increase in

331   temperature as could be observed in Table 1. This increase in oil yield with temperature was

332   as a result to the thermodynamic effect of oil solubilization inside the solid seed particles

333   [32]. The observations in the kinetic parameters of the hyperbolic and Pseudo second order

334   models, were in line with the results obtained by Kitanovic et al. [19] and Agu et al. [56] for

335   the solvent extraction of resinoid from aerial part of *Hypericum perforatum L* and extraction

336   of oil from *Colocynthis vugaris Shrad* seed, respectively.

Table 1: Hyperbolic and Pseudo second order models kinetic parameters for IGK oil extraction at 35, 40, 45, 50 and 55 °C, and oil yields
at 150 min

	35°C					40°C					45°C					50°C					55°C				
	0.5mm	1.0mm	1.5mm	2.0mm	2.5mm	0.5mm	1.0mm	1.5mm	2.0mm	2.5mm	0.5mm	1.0mm	1.5mm	2.0mm	2.5mm	0.5mm	1.0mm	1.5mm	2.0mm	2.5mm	0.5mm	1.0mm	1.5mm	2.0mm	2.5mm
Hyperbolic																									
$\bar{y}_{exp}$	60.08	42.01	39.70	37.18	35.40	62.25	44.15	41.50	39.09	37.78	64.69	46.60	43.90	41.63	39.00	66.70	47.20	45.10	43.15	41.10	68.80	50.20	47.70	45.00	43.00
$\bar{y}_{cal}$	60.26	41.49	39.46	38.16	35.78	62.36	43.35	41.36	39.69	37.24	65.31	45.97	43.31	41.91	39.74	66.56	47.53	45.61	43.63	41.58	68.63	49.91	47.32	45.26	43.58
C_1	4.671	1.844	1.921	1.866	1.541	4.844	2.244	2.219	2.241	1.935	5.289	2.318	2.298	2.349	2.060	5.522	2.576	2.791	2.734	2.449	6.257	2.849	2.977	3.134	2.850
C_2	0.0708	0.0376	0.0420	0.0422	0.0364	0.0710	0.0451	0.0470	0.0498	0.0453	0.0743	0.0438	0.0464	0.0494	0.0452	0.0763	0.0475	0.0545	0.0560	0.0522	0.0845	0.0504	0.0563	0.0626	0.0587
R^2	0.9979	0.9920	0.9923	0.9888	0.9883	0.9974	0.9932	0.9931	0.9916	0.9880	0.9950	0.9938	0.9923	0.9929	0.9899	0.9973	0.9917	0.9972	0.9957	0.9942	0.9967	0.9964	0.9963	0.9954	0.9956
RMS (%)	0.0196	0.0386	0.0375	0.0441	0.0459	0.0220	0.0352	0.0348	0.0380	0.0460	0.0307	0.0334	0.0370	0.0354	0.0418	0.0223	0.0382	0.0224	0.0275	0.0318	0.0249	0.0255	0.0258	0.0280	0.0275
SEE	0.4284	0.5863	0.5461	0.6313	0.6064	0.4881	0.5667	0.5378	0.5715	0.6500	0.7106	0.5671	0.6002	0.5572	0.6254	0.5365	0.6854	0.3759	0.4504	0.4967	0.6108	0.4698	0.4572	0.4831	0.4546
ARE %	1.4134	2.4687	2.3486	1.4811	2.3101	1.4863	2.4892	1.5915	1.7874	3.1997	2.3165	1.7099	2.3369	1.8069	1.6329	1.4461	2.1957	0.2843	1.1166	1.2426	1.5130	1.4500	1.6661	1.5070	1.2685
2nd order																									
$\bar{y}_{exp}$	60.08	42.01	39.70	37.18	35.40	62.25	44.15	41.50	39.09	37.78	64.69	46.60	43.90	41.63	39.00	66.70	47.20	45.10	43.15	41.10	68.80	50.20	47.70	45.00	43.00
$\bar{y}_{cal}$	60.40	41.49	39.27	37.83	35.51	62.55	43.22	41.25	39.42	37.05	65.50	45.86	43.16	41.68	39.44	66.75	47.46	45.46	43.42	41.36	68.88	49.81	47.19	45.06	43.36
C_s	66.810	47.735	44.481	42.079	40.466	69.378	48.913	46.512	43.305	41.497	72.337	52.226	48.508	46.111	43.706	73.529	53.771	50.283	47.566	45.511	75.562	55.866	52.145	48.855	47.170
K	9.4×10^{-4}	9.3×10^{-4}	1.1×10^{-3}	1.4×10^{-3}	1.2×10^{-3}	8.8×10^{-4}	1.0×10^{-3}	1.1×10^{-3}	1.6×10^{-3}	1.3×10^{-3}	8.8×10^{-4}	9.2×10^{-4}	1.1×10^{-3}	1.4×10^{-3}	1.4×10^{-3}	8.9×10^{-4}	9.3×10^{-4}	1.3×10^{-3}	1.5×10^{-3}	1.5×10^{-3}	9.1×10^{-4}	9.8×10^{-4}	1.2×10^{-3}	1.6×10^{-3}	1.6×10^{-3}
R^2	0.9984	0.9943	0.9944	0.9898	0.9914	0.9980	0.9948	0.9943	0.9928	0.9912	0.9963	0.9948	0.9941	0.9943	0.9912	0.9979	0.9926	0.9971	0.9960	0.9948	0.9972	0.9971	0.9972	0.9961	0.9959
RMS (%)	0.0175	0.0349	0.0344	0.0527	0.0469	0.0202	0.0311	0.0329	0.0425	0.0412	0.0265	0.0312	0.0336	0.0365	0.0475	0.0206	0.0361	0.0259	0.0309	0.0356	0.0242	0.0234	0.0234	0.0296	0.0319
SEE	0.3711	0.4957	0.4650	0.6003	0.5212	0.4260	0.4956	0.4895	0.5297	0.5559	0.6107	0.5181	0.5239	0.4977	0.5825	0.4738	0.6461	0.3823	0.4302	0.4702	0.5617	0.4186	0.3973	0.4453	0.4413
ARE %	0.6386	1.1096	0.9599	1.1205	0.0829	0.5053	1.6077	0.7970	0.3582	1.6930	1.3477	0.9898	1.2316	0.1023	0.6683	0.5106	1.7920	0.7151	0.3767	0.4372	0.2921	0.8298	0.8339	0.0376	0.3920

3.3. Degree fitting of the studied kinetic models

The principles for the determination of the model that best fit the experimental data for the two nonlinear models studied were $R^2, RMS, ARE \%$ and SEE. Conventionally, the higher the value of the R^2 and the lower the values of the error estimates (RMS, ARE % and SEE), the better would be the goodness of the model to fit the experimental data [19,56]. Across the various particles sizes and temperatures, the average values of $R^2, RMS, ARE \%$ and SEE evaluated from Table 1 were (0.9937, 0.0326, 1.7628 and 0.5477) and (0.9949, 0.0324, 0.7772 and 0.4940), for hyperbolic and pseudo second order models, respectively. From these values, it could be seen that the RMS average values for both models were all less than ± 5 %, while those of SEE and ARE were all greater than 5 %. Therefore, on the basis of the pseudo second order model's values for $RMS, ARE \%$ and SEE , that were lower than those of hyperbolic model, as well as, its higher R^2 value, pseudo second order model, gave better fit to the experimental kinetic data when compared to the hyperbolic model. As such, pseudo second order model was chosen as a better model for oil extraction from IGK. Similar result was reported by Agu et al. [56] for the modeling of oil extraction from *Colocynthis vugaris Shrad* seed using five different kinetic models.

Furthermore, it could be seen in Table 1 that the experimental and models' calculated oil yields for both hyperbolic and pseudo second order models, were relatively close. For instance, the highest calculated models' oil yields for hyperbolic and pseudo second order, were 68.63 and 68.88 %, respectively. These values were obtained at 55 ° (328 K), 0.5 mm particle size and 150 min. As could be seen in Table 1, these values were very close to the 68.80 % obtained experimentally. This is therefore an indication that both models fit the extraction of oil from IGK using n-hexane as solvent. In other words, variation in particle size, extraction time and temperature, influenced the oil yield significantly, as evident form the obtained results [18,26,57].

3.4. Extraction curves for IGK oil extraction

Fig. 3 shows the increase in IGK oil yield during the extraction of oil from the ground *Irvingia gabonensis* kernel using n-hexane at different particle sizes and extraction temperature. The extraction curve exhibits the shape of a typical soxhlet and batch extractions of substances from plant materials as could be seen in previous works [26,57]. From the curve, it was observed that at a particular temperature, the IGK oil yield increased rapidly at the onset of the extraction, and gradually slows in the later stages. This initial extraction stage was characterized by an exceeding fast extraction rate. This fast extraction rate was due to the exposure of the milled IGK particles to fresh solvent which makes the solubilization of the free oil on the surface of the IGK very easy, and as such, oil was quickly extracted [26]. However, during the later extraction stages, the oil diffused from the interior of the IGK particles and dissolve in the solvent. The oil yield of *Irvingia gabonensis* kernel was found to increase with increase in extraction temperature. This was attributed to better oil solubility at higher temperatures as could be seen in Fig. 3 (a – e) [26]. From Fig 3 a – e, it could be seen that at a particular temperature, higher oil yields were obtained at lower particle size due to bigger interfacial area of the kernel particles [55].
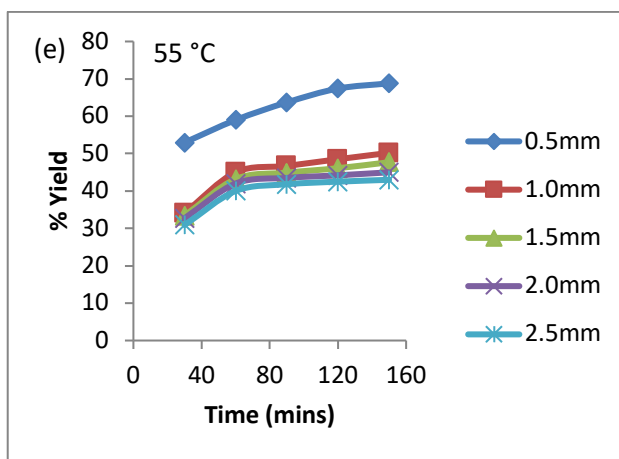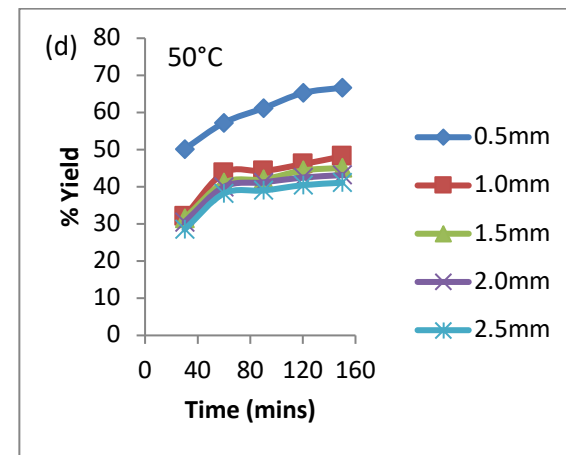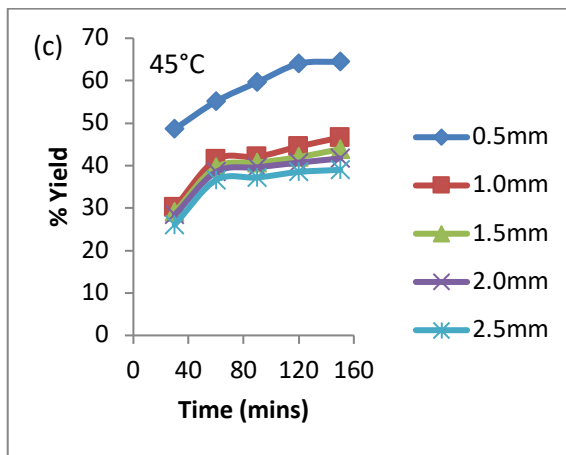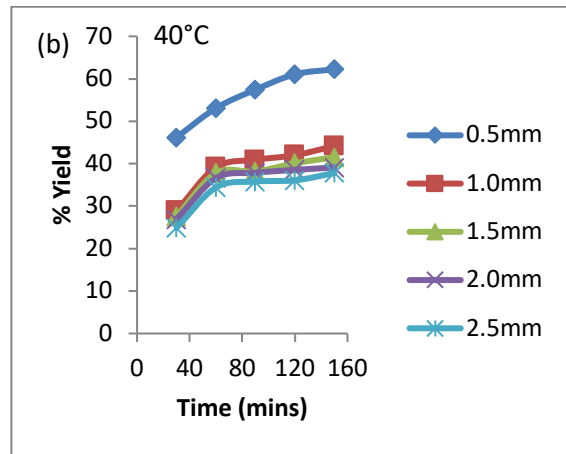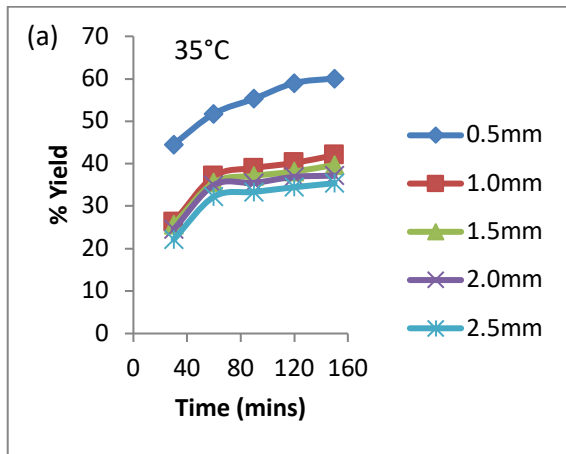
Fig. 3: Extraction curve of *Irvingia gabonensis* kernel oil yield at different particle size diameters, temperatures and time

3.5. Temperature dependence and temperature effects

Fig. 1 (a) to (e) shows the effects of temperature on the oil yield of *Irvingia gabonensis* kernel at particle sizes of 0.5, 1.0, 1.5, 2.0, and 2.5 mm, respectively. Similar to the effect of

time, oil yield increased with increase in temperature from 35 °C to 55 °C. Thus, increasing

the temperature from 35 to 55 °C favors the extraction yield. This is because of the ease of

penetration of the IGK matrix by the already energized n-hexane solvent molecules [58]. This

was also due to the increase in the diffusivity of the IGK oil and decrease in solvent viscosity

at increased temperature. In general, increase in temperature enhances softening of IGK, thus,

improves the mass transfer coefficient of extraction leading to improved extraction oil yield

[59-60].

From the plots in Fig 1 (a – e), it is evident that the extraction process was very fast at the

inception, between 30 and 90 min. Afterwards, it gradually slowed between 90 and 150 min.

This phenomenon was due to internal diffusion. However, the rapid extraction process at the

inception was due to free oil present on the surface of the milled IGK that was exposed to

fresh solvent. Thus, there was easy solubility of the oil in the solvent, which lead to fast

extraction of the oil [26,59]. In this present study, like the previous works in the literature, the

oil yield of IGK increased with temperature and time. The highest oil yield of 68.8 % was

obtained at 55 °C, 150 min and 0.5 mm particle size.

It is important to state at this point that rate of extraction at the very beginning, C_1, and the

constant related to maximum extraction yield, C_2, were determined at different temperatures.

They were dependent on temperature as could be seen in Figs. 4 and 5, respectively. On the

other hand, the extraction capacity, C_s, the second order extraction rate constant, k, and the

initial extraction rate, h, were also determined at different temperatures. They were also

dependent on temperature as evident in Figs. 6, 7 and 8, respectively.
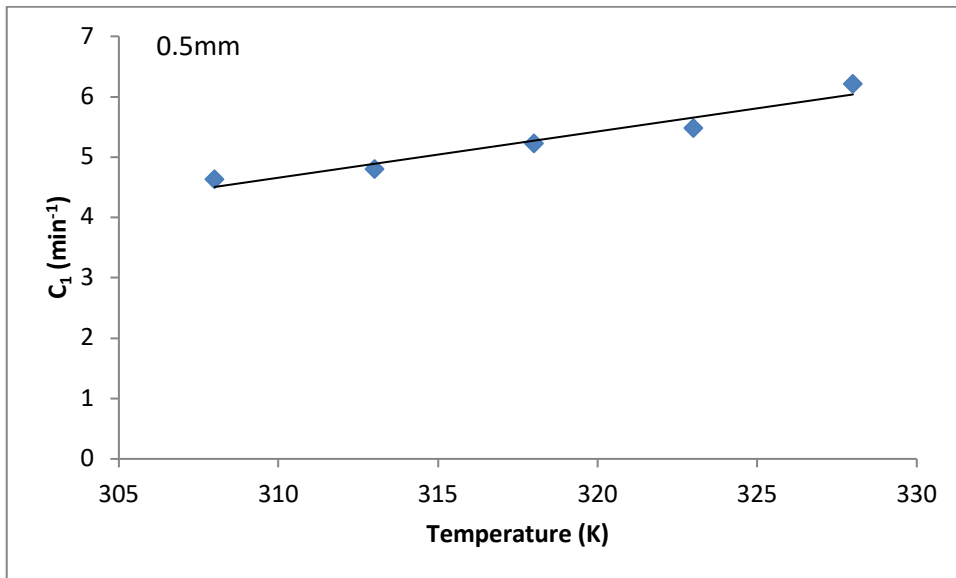
Fig. 4: Relationship between the absolute temperature and the hyperbolic model extraction rate constant at the beginning C_1 for the extraction of oil from *Irvingia gabonensis* kernel at particles size of 0.5mm.
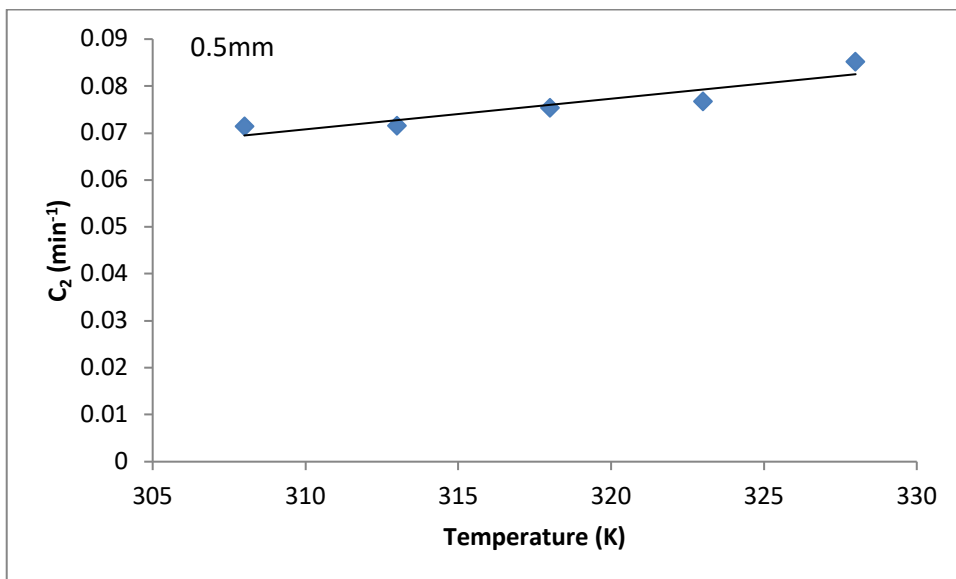

Fig. 5: Relationship between the absolute temperature and the hyperbolic model rate constant related to maximum extraction yield C_2 for the extraction of oil from *Irvingia gabonensis* kernel at particles size of 0.5mm.
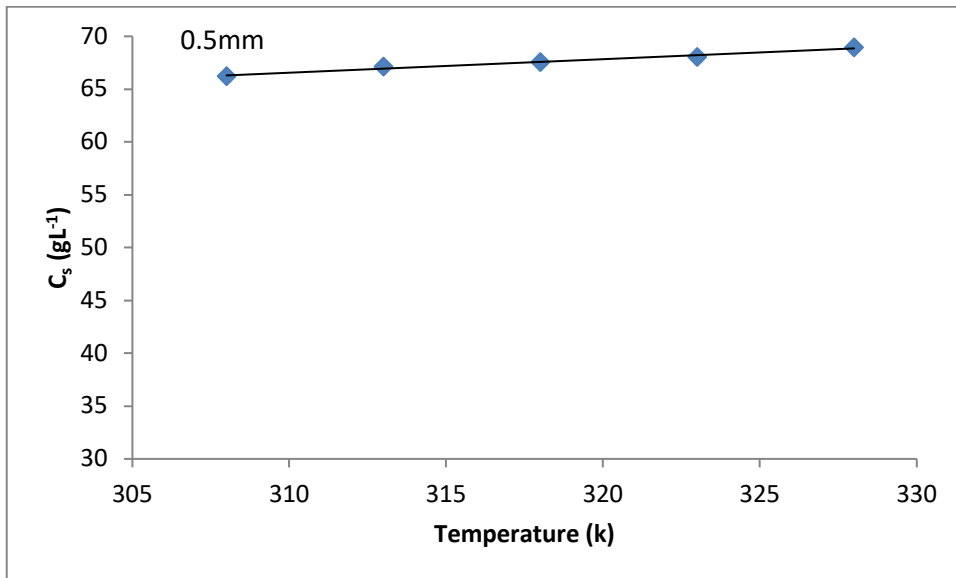
434
435
Fig. 6: Relationship between the absolute temperature and the pseudo second-order extraction capacity constant C_s for the extraction of oil from *Irvingia gabonensis* kernel at particles size of 0.5mm.

439
440
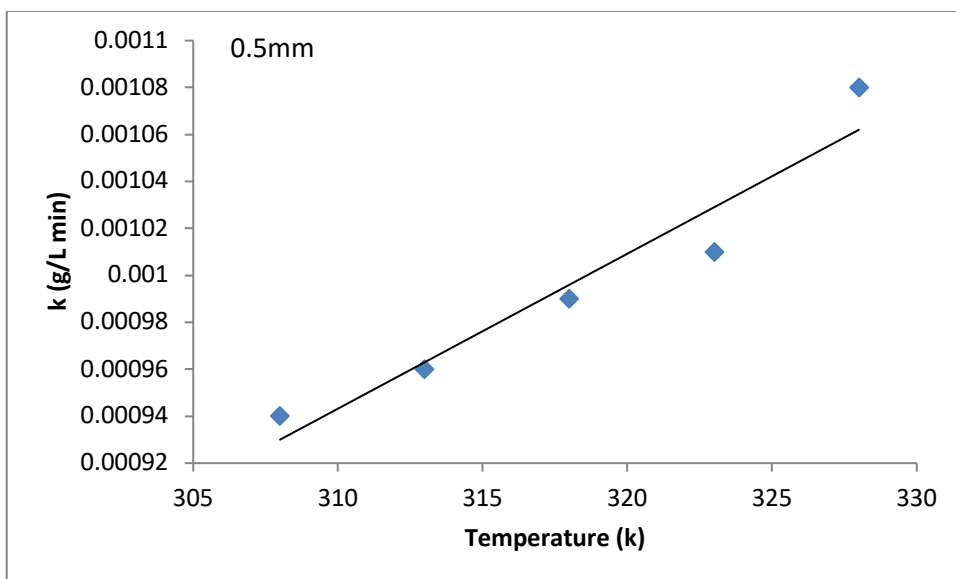
441
442
Fig. 7: Relationship between the absolute temperature and the pseudo second-order extraction rate constant k for the extraction of oil from *Irvingia gabonensis* kernel at particles size of 0.5mm.

446
447
448
449
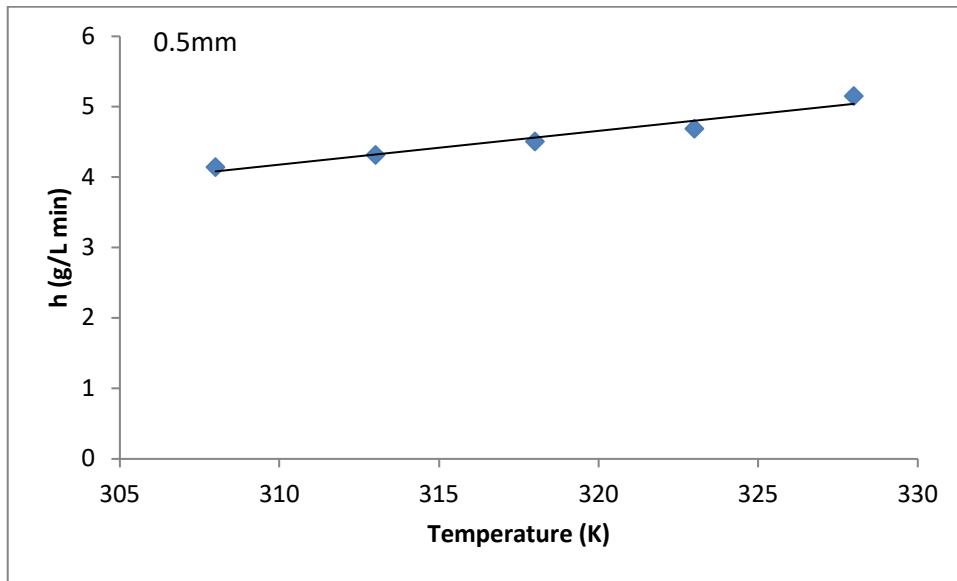
450
451
452 **Fig. 8: Relationship between the absolute temperature and the pseudo second-order**

453 **initial extraction rate h for the extraction of oil from *Irvingia gabonensis* kernel at**

454 **particles size of 0.5mm.**

455 Obviously, the initial extraction rate, C_1, increased with temperature, so did the constant that

456 is related to maximum extraction yield, C_2. Similarly, the initial extraction rate, h, extraction

457 capacity, C_s, and the second-order rate constant, k, all increased with temperature. These

458 findings were in line with the findings of Rakotondramasy et al. [42] for the solid–liquid

459 extraction of protopine from *Fumariaofficinalis* L. It is important to note that when the

460 temperature was kept at 308K, for a particle size of 0.5 mm, the initial extraction rate C_1 for

461 hyperbolic model was 6.21 min^{-1}. This value was slightly higher than 5.15gL^{-1} min^{-1} obtained

462 for the initial extraction rate in pseudo second-order model. On the other hand, the constant

463 related to maximum extraction yield C_2, for hyperbolic model, at the same constant

464 temperature of 308 K and 0.5 mm particle size was 0.085 min^{-1}, while the second-order rate

465 constant, k was 0.0011 Lg^{-1} min^{-1}. However, the extraction capacity, C_s, at the same

466 temperature and particle size was 68.97gL^{-1}. This value was very close to pseudo second-

467   order model calculated oil yield, C_t, 68.52 wt. %. This is an indication of the fitting of the

468   second-order model for the extraction of oil from IGK.

3.6. Activation energy determination

470   The linearized Arrhenius equation [Equation (14)], was used to determine the relationship

471   between k and T, the k_0 and E_a. This was done by plotting In k versus 1000/T for pseudo

472   second-order kinetic model (Fig. 9). The plot shows that the rate constant increases with the

473   increases in temperature. However, a modified form of Arrhenius equation [Equation (25)]

474   was used to determine the relationship between C_2 and T, the k_0 and E_a for hyperbolic kinetic

475   model. Like the pseudo second-order model, this was carried out by plotting In C_2 against

476   1000/T (Fig. 10).

477   $$In\ C_2 = In\ k_0 + \left(-\frac{E_a}{R} \cdot \frac{1}{T}\right) \tag{25}$$

478   Using Equations 14 and 25, activation energies were calculated from the slopes and the

479   values of temperature independent factors calculated from the intercept for the pseudo

480   second-order (Fig. 9) and hyperbolic (Fig. 10) models, respectively. The relationships for the

481   activation energy of extractions at 328K and 2.5 mm particle size, modeled using pseudo

482   second-order and hyperbolic models, are given by Equations (26) and (27), respectively.

483   $$k = k_0\ exp\left(\frac{-11900}{8.314 \times 328}\right) \tag{26}$$

484   $$C_2 = k_0\ exp\left(\frac{-18790}{8.314 \times 328}\right) \tag{27}$$

485   Their respective R^2 values for pseudo second-order and hyperbolic models were 0.9582 and

486   0.9453.

487   In both models, the activation energies were positive, which is an indication that the

488   extraction of oil from IGK is an endothermic process. In the case of pseudo second-order

489   models, the activation energies for average particles size of 0.5, 1.0, 1.5, 2.0 and 2.5 mm

490   were 5.49, 5.57, 5.79, 6.11, and 11.90 kJ/mol, respectively. Similarly, for hyperbolic model,

491   the activation energies at these average particle sizes were 7.03, 11.03, 12.52, 16.63 and

492   18.79 kJ/mol, respectively. These results show that irrespective of the kinetic model used, the

493   rate constants were dependent on the temperature, and they increased with increase in

494   temperature. Also, the rate constants for the models were more temperature sensitive for

495   larger particles size than for the smaller ones. This is manifested in the higher values of the

496   activation energies obtained for larger average particles sizes. This observation is in close

497   agreement to that obtained by Bucic-Kojic et al. [43] for the extraction of polyphenols from

498   grape seeds. Thus, the influence of temperature on the extraction rate constant was more

499   pronounce in larger particles size, than in the smaller ones. Finally, it could be seen that the

500   activation energy values obtained for hyperbolic model at different particles size diameters,

501   were higher than those obtained for pseudo second-order model. This could be attributed to

502   the higher values of the rate constant obtained for hyperbolic model, compared to those

503   obtained for pseudo second-order model [18].
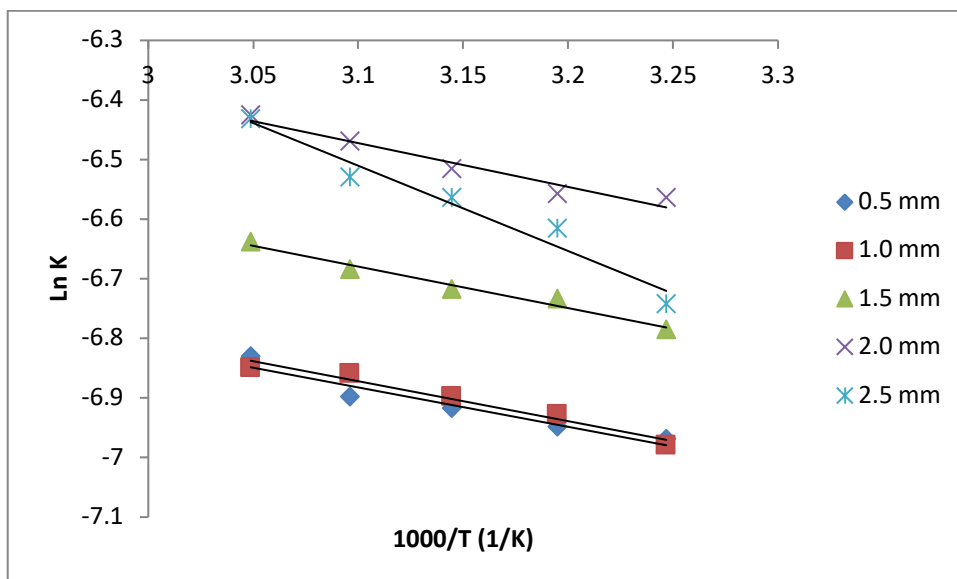
504

505 **Fig. 9: Arrhenius plots for the extraction of oil from *Irvingia gabonensis* kernel at 0.5,**
506 **1.0, 1.5, 2.0 and 2.5 mm particle sizes for pseudo second-order kinetic model.**

507
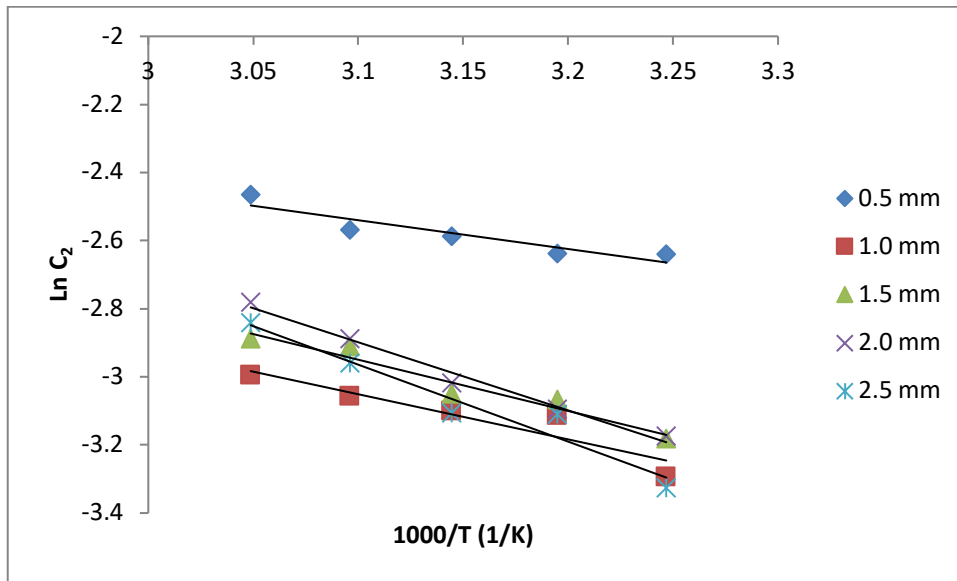
Fig. 10: Arrhenius plots for the extraction of oil from *Irvingia gabonensis* kernel at 0.5, 1.0, 1.5, 2.0 and 2.5 mm particle sizes for hyperbolic kinetic model.

3.7. Modeling

From Equations 7 and 12, the initial extraction rates h and C_1 for pseudo second-order and hyperbolic models, respectively, could be modeled by plotting In h verses 1/T and In C_1 verses 1/T for the respective models. Figs. 11 and 12 show their respective plots. From the plots, the relationships (28) and (29) were established at temperature of 328 K and 2.5 mm particle size.

$$h = k_0 \, exp\left(\frac{-2924}{T}\right) \qquad\qquad (28)$$

$$C_1 = k_0 \, exp\left(\frac{-2913}{T}\right) \qquad\qquad (29)$$

It could be seen that their initial extraction rates where close, although pseudo second-order model had the higher value than that of hyperbolic. This also reflects in the values obtained in Equations (28) and (29).

523
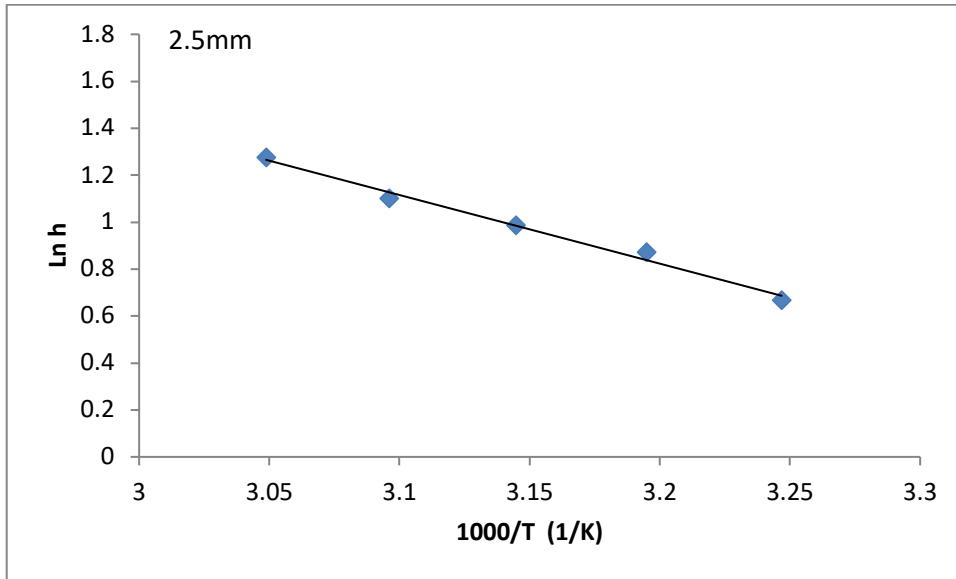
Fig. 11: Relationship between the initial extraction rate, *In* h and temperature, for oil extraction from *Irvingia gabonensis* kernel at 2.5 mm particles size, using pseudo second-order model.

527

528

529
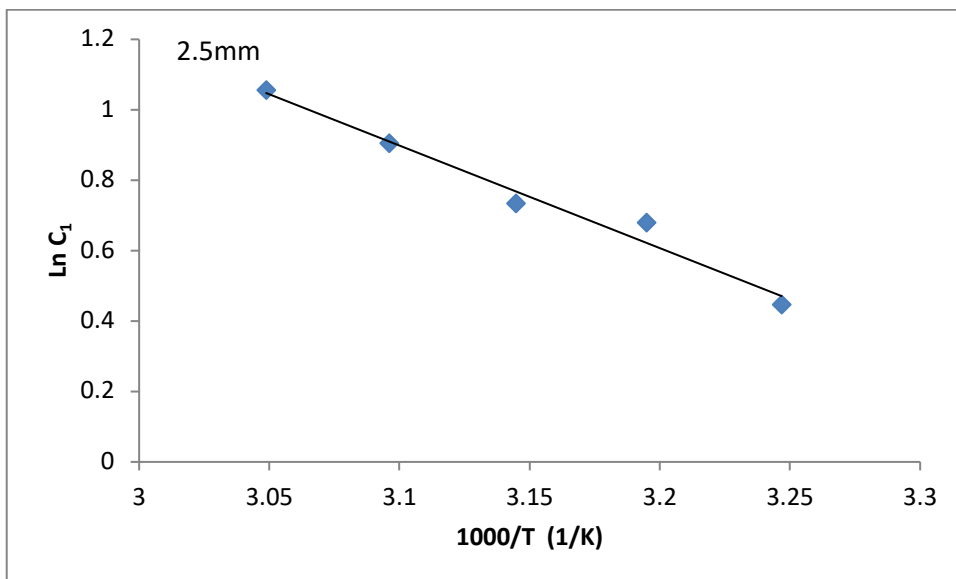
Fig. 12: Relationship between the initial extraction rate, *In* C_1 and temperature, for oil extraction from *Irvingia gabonensis* kernel at 2.5 mm particles size, using hyperbolic model.

For the pseudo second order model, Fig. 13 shows the relationship that exists between extraction capacity, C_s and temperature at particles size of 2.5 mm and the plot lead to Eq. (30).

$$C_s = 0.33T - 59.84 \tag{30}$$

By the combination of equations (13), (28), and (30), the equation that describes the development of C_t versus time and temperature model for pseudo second-order model can be written as Equation (31).

$$C_t = \frac{t}{k_0 \, exp\left(\frac{2942}{T}\right) + \left(\frac{t}{0.33T - 59.84}\right)} \tag{31}$$

This equation shows the model for the evaluation of oil yield during solvent extraction of oil from *Irvingia gabonensis* kernel, for different temperature at any given time, using pseudo second-order model. This equation simply explains that the longer the time of extraction and the higher the extraction temperature are, the higher would be the concentration C_t.
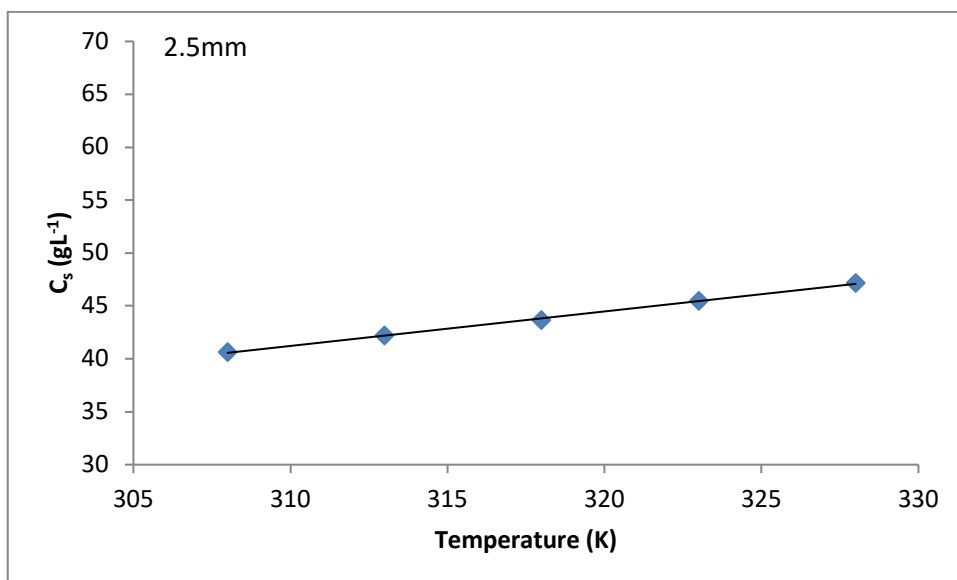

Fig. 13: Relationship between the saturated extraction capacity, C_s, and temperature, for the extraction of oil from *Irvingia gabonensis* kernel at 2.5 mm particles size, using pseudo second order model.

Similarly, Fig. 14 shows the relationship between the constant related to maximum extraction yield C_2 (min^{-1}) and temperature at 2.5 mm particle size. The plot gives rise to equation (32).

$$C_2 = 0.001T - 0.284 \tag{32}$$

The combination of equations (3), (29) and (32), the equation that describes the development of $\bar{y}$ versus time and temperature model for hyperbolic model can be written as Equation (33).

554
$$\bar{y} = \frac{k_0 \, exp\left(\frac{2913}{T}\right)t}{1 + (0.001T^2 - 0.284T)}$$
(33)

555 Similarly, this equation shows the model for the evaluation of oil yield during solvent

556 extraction of oil from *Irvingia gabonensis* kernel, for different temperature at any given time,

557 using hyperbolic model.
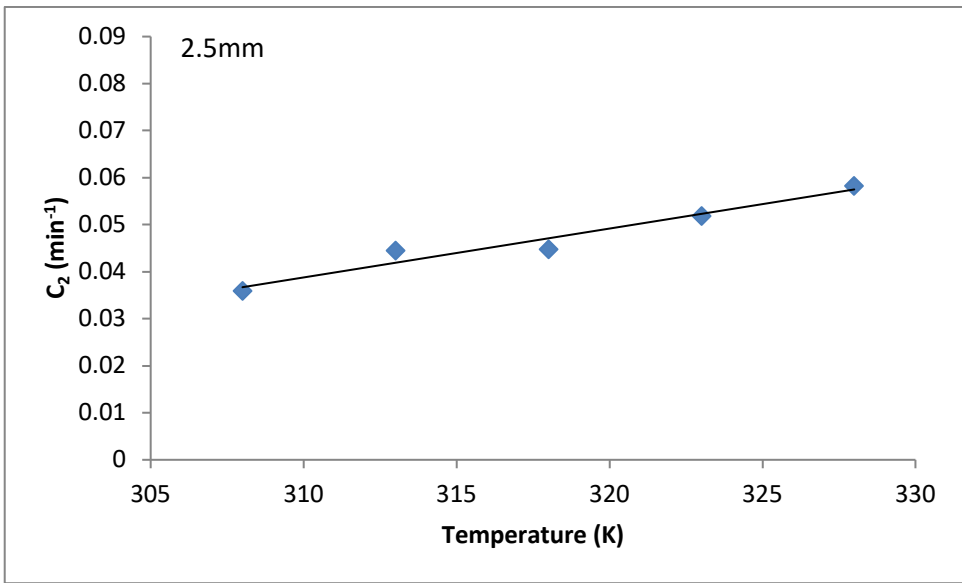
558
559 **Fig. 14: Relationship between the constant related to maximum extraction yield, C_2, and**
560 **temperature, for the extraction of oil from *Irvingia gabonensis* kernel at 2.5 mm**
561 **particles size, using Hyperbolic model.**

562 The models represented by equations (31) and (33) for pseudo second-order and hyperbolic

563 models, respectively, were compared with the experimental data. Fig. 15 shows the

564 comparison between the experimental and the models calculated IGK oil yield at different

565 particle sizes and time, for temperature of 55 °C. From the plots (Fig. 15 and Table 1), good

566 fit between the experimental and the calculated models' data was obtained for both pseudo

567 second-order and hyperbolic models. This is an indication of the validity of the relationships.

568
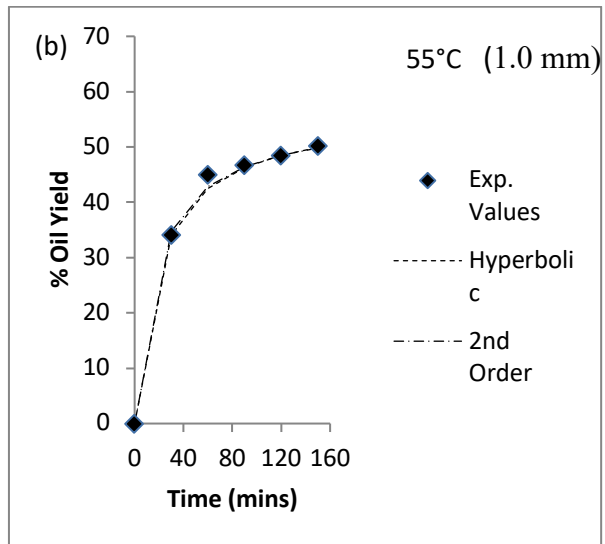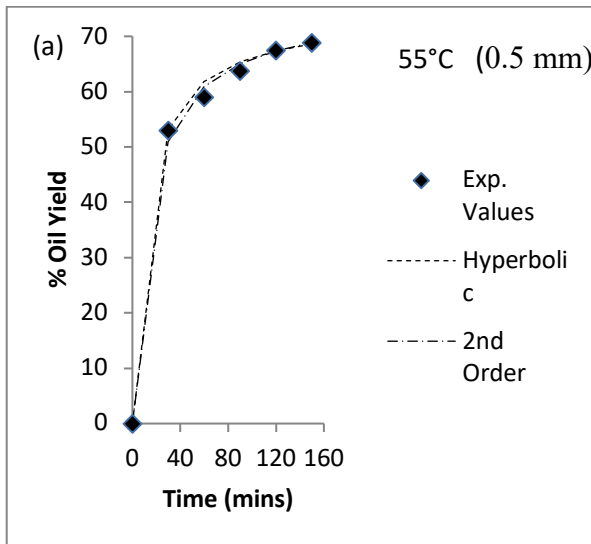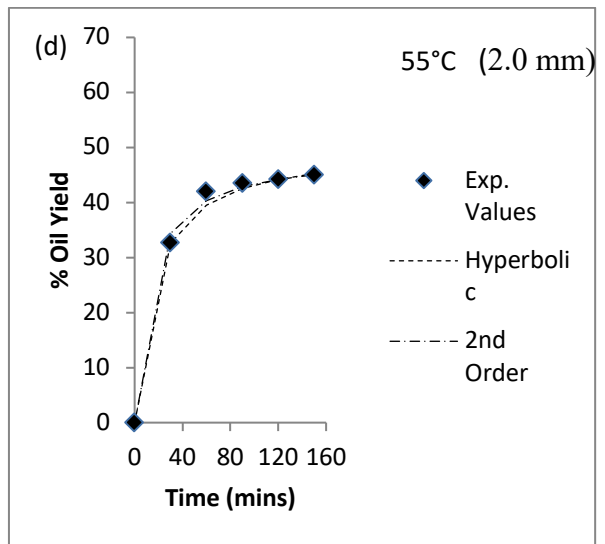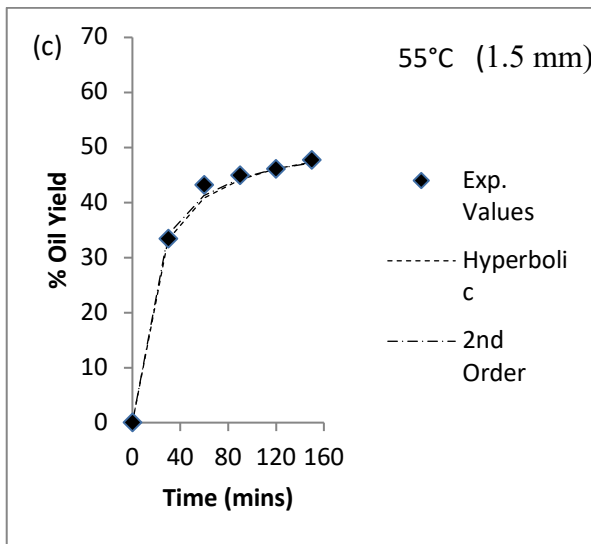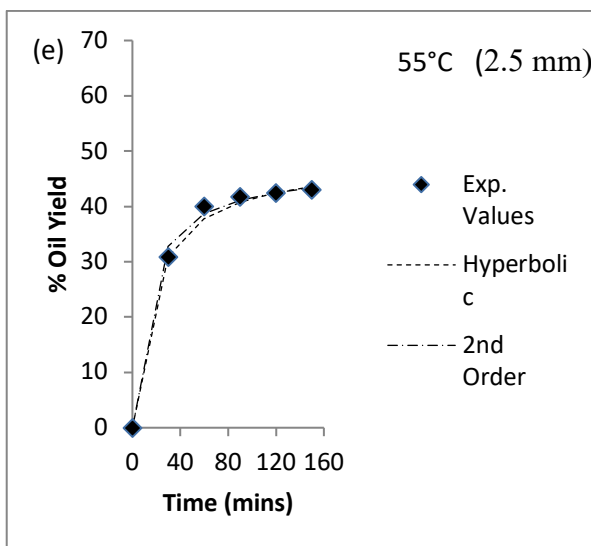
Fig. 15: Comparison between experimental and models' oil yield at different particles sizes and time at 55 °C.

576　Furthermore, Table 1 shows the results of the IGK oil yields obtained at different

577　temperatures and particle size diameter at 150 min, and compared with the calculated models'

578　oil yields values. The compared results of the experimental and calculated models' oil yields

579　data indicate good agreement of the models with the experimental data, as evident from the

580　low error analysis values (Table 1).

581　**3.8. Thermodynamic parameters**

582　The values of the equilibrium constant and other thermodynamic parameters of IGK oil

583　extraction are presented in Table 2. Similarly, the plots of In K verses 1/T for different

584　particles sizes of 0.5, 1.0, 1.5, 2.0 and 2.5 mm, that were used in the determination of

585　thermodynamics parameters (ΔH, ΔS and ΔG) values are shown in Fig. 16. For the

586　thermodynamics of IGK oil extraction, the enthalpy values for the process were in the ranges

587　of 251.81 – 569.28 kJ/mol, for the various particle sizes considered. The enthalpy values for

588　the IGK oil extraction in the present study, were within the ranges (266.18 – 435.87 kJ/mol)

589　and (182.81 – 598.74 kJ/mol) for *Colocynthis vugaris Shrad* seed and *Terminalia catappa*

590　kernel oil extractions, reported by Agu et al. [56] and Menkiti et al [59], respectively.

591　However, the enthalpy result in this work was higher than (4 – 13.5 kJ/mol) reported by

592　Meziane and kadi [61], for olive cake oil. This difference in the enthalpy values was due to

593　seeds morphology, as their morphology often affects oil extraction [56]. The positive values

594　of the enthalpy change are an indication that IGK oil extraction process was endothermic

595　[59]. Similarly, as could be seen in Table 2, the entropy change of the process was also

596　positive. The entropy values for IGK oil extraction ranged between 1.08 – 1.99 kJ/mol, with

597　larger IGK particle sizes having higher entropy change values. The implication of this

598　positive entropy values is that the process was irreversible in nature [26,61]. For the Gibbs

599　free energy change values of the process, the entire values were negative. Hence, this is an

600　indication of the feasibility and spontaneous nature of the process. From Table 2, it could be

601 seen that the ΔG values were highly negative and in the range of -43.22 to -105.49 kJ/mol.

602 This relatively high negative value(s) of ΔG is an indication that the extraction process was

603 highly spontaneous [26,56].
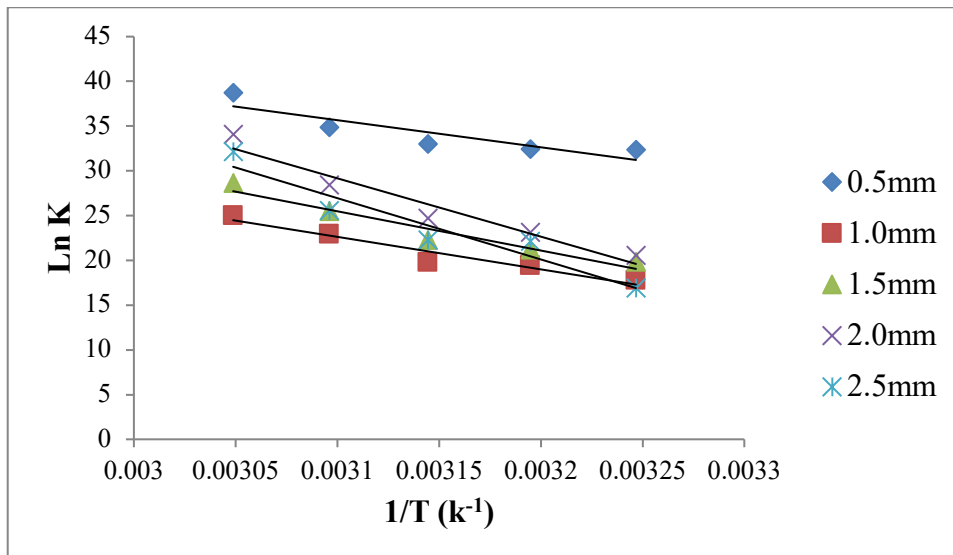
604
605 **Fig. 16: Plot of In K (equilibrium constant) vs. 1/T (temperature, K^{-1}) for the five**
606 **different particle sizes.**

607 **Table 2: Thermodynamic parameters for the extraction of IGK oil n-hexane**

T	0.5mm				1.0mm				1.5mm				2.0mm				2.5mm			
(K)	K	ΔH KJ/mol	ΔS KJ/mol	ΔG KJ/mol	K	ΔH KJ/mol	ΔS KJ/mol	ΔG KJ/mol	K	ΔH KJ/mol	ΔS KJ/mol	ΔG KJ/mol	K	ΔH KJ/mol	ΔS KJ/mol	ΔG KJ/mol	K	ΔH KJ/mol	ΔS KJ/mol	ΔG KJ/mol
308	1.10×10^{14}			-82.80	4.87×10^{7}			-45.33	4.07×10^{8}			-50.77	8.14×10^{8}			-52.54	2.14×10^{7}			-43.22
313	1.21×10^{14}			-84.39	2.70×10^{8}			-50.52	1.57×10^{9}			-55.10	1.10×10^{10}			-60.16	3.92×10^{9}			-57.48
318	2.16×10^{14}	251.81	1.08	-87.27	3.69×10^{8}	302.01	1.12	-52.15	4.53×10^{9}	364.60	1.34	-58.78	5.11×10^{10}	541.57	1.92	-65.19	4.66×10^{9}	569.28	1.99	-58.86
323	1.38×10^{15}			-93.61	8.88×10^{9}			-61.51	1.14×10^{11}			-68.36	2.19×10^{12}			-76.31	1.26×10^{11}			-68.63
328	6.31×10^{16}			-105.49	7.02×10^{10}			-68.11	2.59×10^{12}			-77.95	6.13×10^{14}			-92.88	9.04×10^{13}			-87.63

608

3.9. Physicochemical properties of *Irvingia gabonensis* kernel oil (IGKO)

The physicochemical characteristics of IGKO are shown in Table 3. In terms of IGK oil yield, it was found to be 68.80% (by weight) (see Table 3). This value was higher than oil yield values reported for cottonseed [62], and soybean [63], hence, an indication of its economic benefit and possible industrial application of IGKO. As a result, IGKO could constitute an alternative source of oil for industrial application due to its relatively high oil yield. Similarly, Matos et al. [12] and Zoué et al. [11], reported 73.83 % (in mass) and 69.76 % (in mass), respectively, for *Irvingia gabonensis* kernel oil. These values were higher than that obtained in this work. The variation in the IGKO yield in this work when compared to those in the literature could be linked to the extraction methods and conditions, in addition to the type of solvent used [56]. Also, this difference in IGKO yield could also be attributed to factors like, geographical location, seed variety and period of harvest [59,64]. From Table 3, it would be seen that the viscosity and acidity of IGKO were 19.37 $mm^2 S^{-1}$ and 5.18 mg KOH/g, respectively. However, the value of the viscosity in this work was found to be lower than 45 $mm^2 S^{-1}$ for *Irvingia gabonensis* kernel oil, but higher than 3.2 $mm^2 S^{-1}$ for the IGK oil biodiesel, as reported by Bello et al. [15]. For the acid value, the IGKO acid value (5.18 mg KOH/g) in this work was found to be lower than 9.40 mg KOH/g, reported by Etong et al. [65], but higher than 4.67 mg KOH/g and 1.2 mg KOH/g, reported by Zoué et al. [11] and Bello et al. [15], respectively. As already stated, the difference in the viscosity and acidity of IGKO in this work when compared to those reported elsewhere could be attributed to the breed of *Irvingia gabonensis* kernel used [56,59]. This difference in viscosities of IGKO in this work and those in the literature could be due to differences in the extraction temperatures, since temperature significantly affects viscosity [58]. As could be seen in Table 3, the iodine value (IV) of the IGKO (98.75 $g/I_2/100g$ oil) in this work was higher than the 32.43 $g/I_2/100g$ oil and 4.17 $g/I_2/100g$ oil reported by Zoué et al. [11] and Yusuf et al. [66],

respectively. The high iodine values of the oil are an indication of the high level of unsaturation nature of the oils. As evident in Table 3, the density and moisture content of IGKO were 900 g/cm^3 and 3.75 mg kg^{-1}, respectively. This density was lower than 930 g/cm^3, reported by Bello et al. [15]. In case of moisture content, that of IGKO was higher than 0.023 reported by Matos et al. [12]. The difference in the moisture content could be attributed to the initial moisture content of the IGK sample prior to the extraction process, as well as the method of extraction used [67]. Furthermore, the pour and flash points values of IGKO were 17 °C and 285 °C, respectively (see Table 3). These values were lower than 28 °C and 300 °C, respectively, reported by Bello et al. [15] for IGKO. However, the pour point value IGKO was lower than the pour point (-6 °C) values of *Irvingia gabonensis* kernel oil biodiesel, while its flash point was higher than that of *Irvingia gabonensis* kernel oil biodiesel (140 °C) [15]. This high flash point of IGKO in this work is an indication of the safety handling nature of the oil, hence, could easily be stored at room temperature [68]. The dielectric strength (DS) value of *Irvingia gabonensis* kernel oil (IGKO) was 25.83 KV (Table 3). This value was found to be lower than those of soybean oil (39 KV) [69] and *Terminalia catappa* kernel oil (30.61 KV) [59], but slightly higher than that of palm kernel oil (25 KV) [69]. Although this value is lower than the minimum requirement of 40 to 60 KV for conventional mineral transformer oil, it is important to know that the DS value of IGKO could as well be improved with further purification and transesterification [70].

Table 3: Physicochemical properties of IGK oil

Oil property	Unit	IGKO	Standard method
Oil Yield	%	68.80	AOAC 920.85
Dielectric strength	KV	25.83	IEC 60156
Moisture content	mg kg^{-1}	3.75	AOAC 926.12
Pour point	°C	17	AOCS 969.17
Flash point	°C	285	ASTM D93
Density, 20°C	g cm^{-3}	900	ASTM D1298
Viscosity, 40 °C	mm^2 s^{-1}	19.37	ASTM D93
Acidity/Acid value	mg KOH/g	5.18	AOAC 969.17
Iodine value	g/I$_2$/100g oil	98.75	AOAC 993.20

3.10. FTIR Analysis of *Irvingia gabonensis* Kernel Oil (IGKO)

The result in Fig. 17 was analyzed and compared with known signature of identified materials in the FTIR library [71]. For the IGKO sample (Fig. 17), the peak center at 900.7966 cm^{-1} is characteristics of P – F stretching, indicating the presence of phosphorus compounds. The peak at 1047.5 cm^{-1} is a characteristic of C – O stretching, indicating the presence of alcohol and phenol, which are oxygen-containing compounds. For the peak at 1369.536 cm^{-1}, it is a characteristic of aromatic nitro compound NO$_2$ stretching, which is an indication of the presence of nitrogen-containing compounds. The peaks centers at 1473.258 cm^{-1}and 1664.323 cm^{-1}, are characteristics of C = C stretching and nitrite N – O stretching, respectively, indicating the presence of aromatic compounds and nitrogen-containing compounds, respectively. In a similar way, the peak at 2020.284 cm^{-1} is characteristics of combination N – H stretching, combination O – H stretching, indicating the presence of organic compounds. The peaks at 2353.372 cm^{-1} and 2659.711 cm^{-1} are characteristics of phosphorus acid/ester P – H stretching and phosphorus acid/ester O – H stretching, respectively, which are indications of the presence of phosphorus compounds. Also, the peaks centered at 3002.457 cm^{-1} and 3289.143 cm^{-1} are characteristic of O – H stretching, indicating the presence of carboxylic acids, which are oxygen-containing compounds and

water. Lastly, the peak at 3772.403 cm^{-1} is beyond the infrared band of 3700 wavenumber (cm^{-1}) for organic compounds as such, could not be identified.
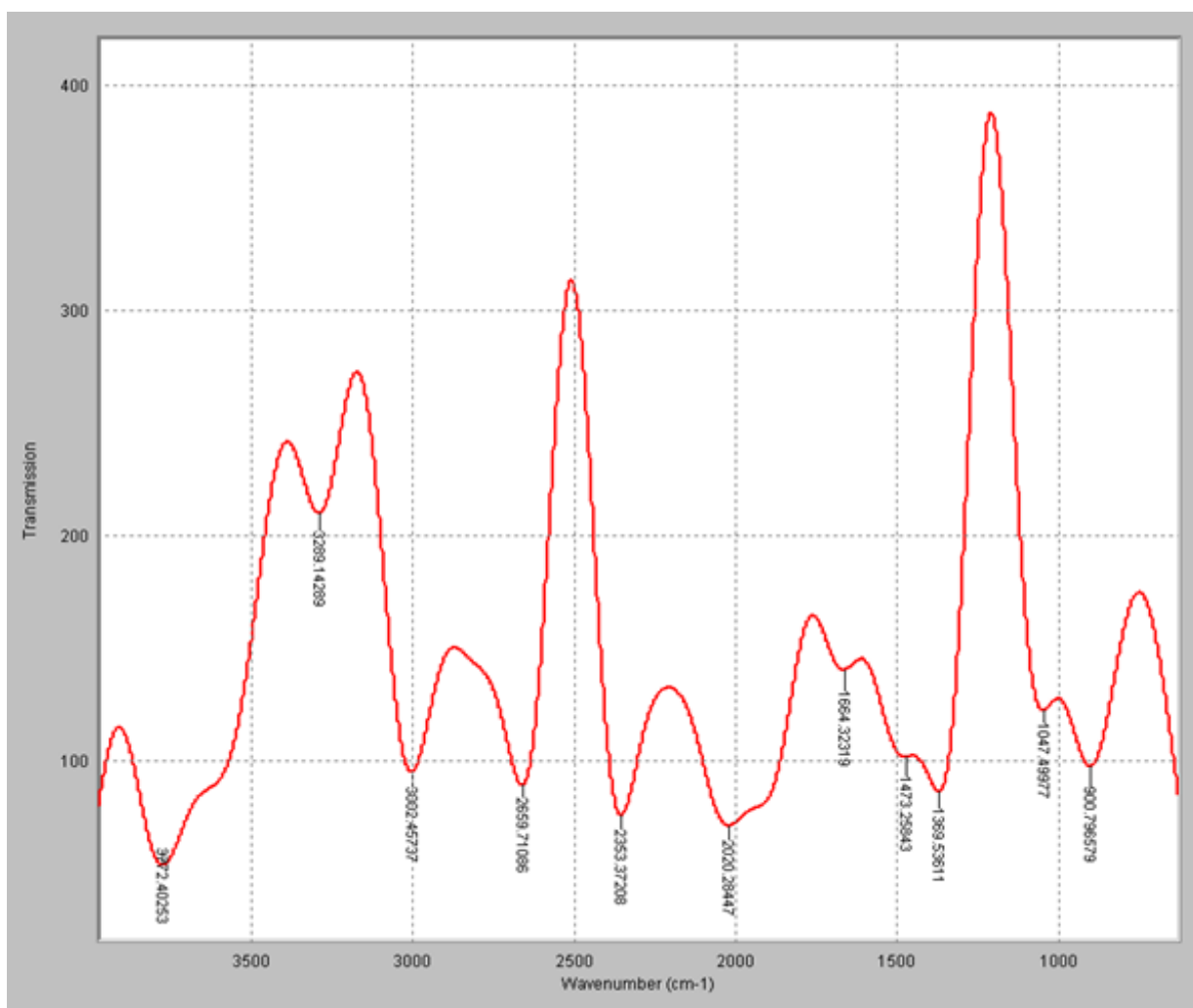
Fig. 17: FTIR spectrum of IGKO.

4. Conclusion

In this work, it has been established that process parameters (temperature, time and particles size), influenced the IGK oil yield. This is due to the fact that increases in temperature and time resulted in the increase in the IGK oil yield, while smaller particle size gave higher IGK oil yield. The highest oil yield of 68.80 % was obtained at 55 °C, 150 min., and 0.5 mm particle size. The physicochemical properties of the IGK oil indicated its potential for use as transformer fluid upon further treatment. Of the two kinetic models studied, pseudo second order gave better fitting to the experimental data than hyperbolic model. The activation

energies determined using Arrhenius equation and modified form of Arrhenius equation for pseudo second order and hyperbolic models, respectively, were all positive, an indication that oil extraction from IGK is an endothermic process. The obtained results indicate that irrespective of the model used, the rate constant k and the constant related to maximum extraction yield C_2, for pseudo second order and hyperbolic models, respectively were temperature dependent, as they increased with temperature increase. Also, the constants k and C_2 for pseudo second order and hyperbolic models respectively were more temperature sensitive for larger particles size than for the smaller ones. This is manifested in the higher values of the activation energies obtained for larger average particles sizes. Kinetic models equations were successfully developed to describe the IGK oil extraction processes under the different process parameters (temperature, time and particle size) for both models. Finally, the ΔG, ΔS and ΔH values obtained at the different particles sizes during the extraction indicated that the process was spontaneous, irreversible and endothermic.

Acknowledgement

Conflict of Interest statement

Authors have no conflict of interest relevant to this article.

References

[1] Ite, A.E., Ibok, U.J., Ite, M.U., Petters, S.W. Petroleum Exploration and Production: Past and Present Environmental Issues in the Nigeria's Niger Delta. American Journal of Environmental Protection, 2013, 1(4), 78 – 90.

[2] Pearson, S.R.Petroleum and the Nigerian Economy: Stanford University Press, 1970.

[3] Manyong, V.M., Ikpi, A., Olayemi, J.K., Yusuf, S.A., Omonona, B.T., Okoruwa, V., Idachaba, F.S. Agriculture in Nigeria: Identifying opportunities for increased commercialization and Investment. International Institute of Tropical Agriculture (IITA), 2005 Ibadan, Nigeria.

[4] Joseph, J.K. Physic-chemical attributes of wild mango (*Irvingia gabonensis*) seeds. Bioresource Technology, 1995, 53, 179 – 181.

[5] Etebu, E. Postharvest pathology and phytochemicals of *Irvingia gabonensis* (Aubry-Lecomte ex O'Rorke) fruits and wastes. Agricultural Science Research Journal, 2012, 2(6), 285 – 294.

[6] Agbogidi, O.M., Okonta, B.C. Role of women in community forestry and environmental conservation. In: Proceedings of FAN Conference held in Calabar. Akindele S. A and Popoola L (eds), 6-11th Oct., 2003, 159 – 163.

[7] Leakey, R.R.B., Greenwell, P., Hall, M.N., Atangana, A.R., Usoro, C., Anegbeh, P.O., Fondoun, J-M., Tchoundjeu, Z. Domestication of *Irvingia gabonensis*: 4. Tree-to-tree variation in food-thickening properties and in fat and protein contents of dika nut. Food Chemistry, 2005, 90, 365–378.

[8] Leakey, R.R.B., Schreckenberg, K., Tchoundjeu, Z. The potential relevance in Latin America of the West African experience with participatory domestication of indigenous fruits. International Forestry Review, 2003, 5, 338–347.

[9] Ayuk, E.T., Duguna, B., Kengue, J., Mouet, M., Tiki Mango T., Zenkeng, P. Uses,

management and economic of *Irvingia gabonesis* in the humid lowlands of Cameroon. Forest Ecological Management, 1999, 113, 1 – 9.

[10] Etta, H.E., Olisaeke, C.C., Iboh, C.I. Effect of *Irvingia gabonensis* (Aubry-Lecomte ex O'Rorke) Seeds on the Liver and Gonads of Male Albino Rats. Journal of Biology, Agriculture and Healthcare, 2014, 4(1), 10 – 15.

[11] Zoueˊ, L.T., Bedikou, M.E., Faulet, B.M., Gonnety, J.T., Niamkeˊ, S.L. Characterisation of highly saturated *Irvingia gabonensis* seed kernel oil with unusual linolenic acid content. Food Science and Technology International, 2013, 19(1), 79 – 87.

[12] Matos, L., Nzikou, J.M., Matouba, E., Pandzou-Yembe, V.N., Mapepoulou, T.G., Linder M., Desobry S. Studies of *Irvingia gabonensis* seeds kernels: Oil technological applications. Pakistan Journal of Nutrition, 2009, 8(2), 151 – 157.

[13] Ngondi, J.L., Oben, J.E., Minka, S.R. The effect of *Irvingia gabonensis* seeds on body weight and blood lipids of obese subjects in Cameroon. Lipids in health and Disease, 2005, 4, 12 – 15.

[14] Shiembo, P.N., Newton, A.C., Leakey, R.R.B. Vegetative propagation of *Irvingia gabonensis*, a West African fruit tree. Forest Ecology and Management, 1996, 87, 185 – 192.

[15] Bello, E.I., Fade-Aluko, A.O., Anjorin, S.A., Mogaji, T.S. Characterization and evaluation of African bush mango Nut (Dika nut) (*Irvingia gabonensis*) oil biodiesel as alternative fuel for diesel engines. Journal of Petroleum Technology and Alternative Fuels, 2011, 2(9), 176 –180.

[16] Omeh, Y.S., Ezeja, M.I., Ugwudike, P.O. The Physiochemical properties and fatty acid profile of oil extracted from *Irvingia gabonensis* seeds. International Journal of Biochemistry and Biotechnology, 2012, 2(2), 273 – 275.

[17] Ekpe, O.O., Umoh, I.B., Eka, O.U. Effect of a typical rural processing method on the

proximate composition and amino acid profile of bush mango seeds (*Irvingia gabonensis*). African Journal of Food Agriculture, 2007, 52, 164–171.

[18] Agu, C.M. Synthesis and Modification of Selected Vegetable Oils for Transformer Oil Production Ph.D thesis. Department of Chemical Engineering, Faculty of Engineering Nnamdi Azikiwe University, Awka, Anambra State, Nigeria, March, 2019.

[19] Kitanovic, S., Milenovic, D., Veeljkovic, V.B. Empirical Kinetic Models for the resinoid extraction from aerial parts of St John's Wort (*Hypericum Perforatum L.*). Journal of Biochemical Engineering, 2008, 41, 1 – 11.

[20] Wang, L., Weller, C.L. Recent advances in the extraction of nutraceuticals from plants. Trends in Food Science and Technology, 2006, 17, 300 – 312.

[21] Reyes-Jurado, F., Franco-Vega, A., Remirez-Crona, N., Palou, E., Lopez-Malo, A. Essential Oils: Activities, Extraction Methods, and their Modeling. Food Engineering Review 2014; (10).

[22] Delgado, T., Malheiro, R., Pereira, J., Ramalhosa, E. Hazelnut (*Corylus avellana L.*) kernels as a source of antioxidants and their potential in relation to other nuts. Industrial Crops and Products, 2010, 32, 621–626.

[23] Saloua, F., Eddine, N.I., Hedi, Z. Chemical composition and profile characteristics of Osage Orange *Maclura pomifera* (Rafin.) Schneider seed and seed oil. Industrial Crop and Products, 2009, 29, 1–8.

[24] Bachheti, R.K., Rai, I., Joshi, A., Rana, V.,. Physico-chemical study of seed oil of *Prunus armeniaca L.* grown in Garhwal region (India) and its comparison with some conventional food oils. International Food Research Journal, 2012, 19(2) 577 – 581.

[25] Niu, L., Li, J., Chen, M., Xu, Z. Determination of oil contents of Sacha inchi (*Plukenetia volubilis*) seeds at different developmental stages by two methods: Soxhlet extraction and time-domain nuclear magnetic resonance. Industrial Crops and Products, 2014, 56,

187–190.

[26] Sulaiman, S., Abdul Aziz, A.R., Aroua, M.K. Optimization and modeling of extraction of solid coconut waste oil. Journal of Food Engineering, 2013, 114, 228–234.

[27] Fernandez, M.B., Perez, E.E., Crapiste, G.H., Nolasco, S.M. Kinetics study of canola oil and tocopherol extraction: parameter comparaison of nonlinear models. Journal of Food Engineering, 2012, 111, 682 – 689.

[28] Amin, S. K., Hawash, S., El Diwani, G., El Rafei, S. Kinetics and thermodynamics of oil extraction from *Jatropha curcas* in Aqueous Acidic Hexane Solution. Journal of American Science, 2010, 6(11), 293 – 300.

[29] Topallar, H., Gecgel, U. Kinetics and thermodynamics of oil extraction from sunflower seeds in the presence of Aqueous Acidic Hexane Solution. Turkish Journal of Chem., 2000, 24, 247 – 253.

[30] Brătfălean, D., Cristea, V.M., Agachi, P.Ş., Irimie, D.F. Improvement of Sunflower oil Extraction by Modelling and Simulation. Revue Roumaine de Chimie, 2008, 53(9) 881–888.

[31] Nwabanne, T.J. Kinetics and Thermodynamics study of oil extraction from fluted Pumpkin seed. International Journal of Multidisciplinary Sciences and Engineering, 2012, 6, 11 – 15.

[32] Liauw, M.Y., Natan, F.A., Widiyanti, P., Ikasari, D., Indraswati, N., Soetaredjo, F.E. Extraction of Neem oil (*Azadirachta indica A. Juss*) using N-hexane and Ethanol: Studies of Oil Quality, Kinetic and Thermodynamic. ARPN Journal of Engineering and Applied Sciences, 2008, 3, 49 – 54.

[33] Mezzomo, N., Martínez, J., Ferreira, S.R.S. Supercritical fluid extraction of peach (Prunus persica) almond oil: Kinetics, mathematical modeling and scale-up. Journal of Supercritical Fluids, 2009, 51, 10–16.

[34] Matthäus, B., Brühl. Comparison of different methods for the determination of the oil content in oilseeds. Journal of the American Oil Chemists Society, 2001, 78, 95 – 102.

[35] Nei, N.H.Z., Fatemi, S., Mehrnia, M.R., Salimi, A. Mathematical modeling and study of mass transfer parameters in supercritical fluid extraction of fatty acids from Trout powder. Biochemical Engineering Journal, 2008, 40, 72 – 78.

[36] Chung, C.A. Simulation Modeling Handbook. A practical Approach. CRC Press, 2004.

[37] Meziane, S., Kadi, H., Daoud, K., Hannane, F. Application of experimental design method to the oil extraction from olive cake. Journal of Food Processing and Preservation, 2009, 33, 176 – 185.

[38] Perez, E.E., Carelli, A.A., Crapiste, G.H. Temperature-dependent diffusion coefficient of oil from different sunflower seeds during extraction with hexane. Journal of Food Engineering, 2011, 105, 180 – 185.

[39] Baümler, E.R., Crapiste, G.H., Carelli, A.A. Solvent extraction: kinetic study of major and minor compounds. Journal of the American Oil Chemists' Society, 2010, 87, 1489 – 1495.

[40] Xiao, X., Song, W., Wang, J., Li, G. Microwave-assisted extraction performed in low temperature and in vacuo for the extraction of labile compounds in food samples. Anal. Chim.Acta, 2012, 712(0), 85–93.

[41] Peleg, M. An empirical model for the description of moisture sorption curves. Journal of Food Science, 1988, 53, 1216–1219.

[42] Rakotondramasy-Rabesiaka, L., Havet, J.-L., Porte, C., Fauduet, H. Solid–liquid extraction of protopine from *Fumariaofficinalis* L. – Analysis determination, kinetic reaction and model building. Seperation, Purification Technology, 2007, 54(2), 253–261.

[43] Bucic-Kojic, A., Planinic, M., Tomas, S., Bilic, M., Velic, D. Study of solid–liquid

extraction kinetics of total polyphenolsfrom grape seeds. Journal of Food Engineering, 2007, 81(1), 236–242.

[44] Chan, C., Yusoff, R., Ngoh, G. Modeling and kinetics study of conventional and assisted batch solvent extraction. Chemical Engineering Research and Design, 2014, 92, 1169 – 1186.

[45] Qu, W., Pan, Z., Ma, H. Extraction modeling and activities of antioxidants from pomegranate marc. Journal of Food Engineering, 2010, 99, 16 – 23.

[46] Rakotondramasy-Rabesiaka, L., Havet, J.L., Porte, C., Fauduet, H. Solid–liquid extraction of protopine from *Fumaria officinalis* L. – Kinetic modelling of influential parameters. Industrial Crops and Products, 2009, 29 (2–3), 516–523.

[47] Alirezaei, M., Zare, D., Nassiri, S. Application of computer vision for determining viscoelastic characteristics of date fruits. Journal of Food Engineering, 2013, 118, 326 – 332.

[48] AOAC. Official methods of Analysis, 15th edition, Association of Official Analytical Chemists, Washington, DC, 1990.

[49] ASTM D445. Standard Test Method for Kinematic Viscosity of Transparent and 451Opaque Liquids (and Calculation of Dynamic Viscosity) 2011.

[50] IEC 60156. Insulating liquids –Determination of the breakdown 487 voltage at powerfrequency–Test method Third edition 2003; 11.

[51] Rathod, V.K., Vetal, M.D., Lade, V.G. Extraction of ursolic acid from Ocimum sanctumvleaves: Kinetics and modeling. Food and Bioproducts Processing, 2012, 90, 793 – 798.

[52] Eikani, M.H., Golmohammad, F., Homami, S.S. Extraction of pomegranate (Punica granatum L) seed oil using superheated hexane. Food and Bioproducts Processing, 2012, 90(1), 32 – 36.

[53] Sayyar, S., Abidin, Z.Z., Yunus, R., Muhammad, A. Extraction of oil from jatropha seeds-optimization and kinetics. American Journal of Applied Sciences, 2009, 6(7), 1390 – 1395.

[54] Sirisompong, W., Jirapakkul, W., Klinkesorn, U. Response surface optimization and characteristics of rambutan (Nephelium lappaceum L.) kernel fat by hexan extraction. LWT – Food Science and Technology, 2011, 44(9), 1946 – 1951.

[55] Huang, Z., Yang, M.-J., Liu, S.-F., Ma, Q. Supercritical carbon dioxide extraction of Baizhu: Experiments and modeling. The Journal of Supercritical Fluids, 2011, 58, 31 – 39.

[56] Agu, C.M., Kadurumba, C.H., Agulanna, A.C., Aneke, O.O., Agu, I.J., Eneh, J.N. Nonlinear Kinetics, Thermodynamics, and parametric studies of *Colocynthis vugaris Shrad* seeds oil extraction. Industrial Crops and Products, 2018, 123, 386 – 400.

[57] Kostic, M.D., Jokovic, N.M., Stamenkovic, O.S., Rajkovic, K.M., Milic, P.S., Veljkovic, V.B. The kinetics and thermodynamics of hempseed oil extraction by n-hexane. Industrial Crop and Products, 2014, (52), 679 – 686.

[58] Ibemesi, J., Attah, J. Temperature effects on the extraction of rubber and melon seed oils. Journal of the American oil Chemists' Society, 1990, 67(7), 443-445.

[59] Menkiti, M.C., Agu, C.M., Udeigwe, T.K. Extraction of oil from Terminalia catappa L.: Process parameter impacts, kinetics and thermodynamics. Industrial Crop and Products, 2015, 77, 713 – 723.

[60] Tao, Y., Zhang, Z., Sun, D. Kinetics modeling of ultrasound-assisted extraction of phenolic compounds from grape marc: Influence of acoustic energy density and temperature. Ultrasonics Sonochemistry, 2014, 21, 1461 – 1469.

[61] Meziane, S., Kadi, H. Kinetics and thermodynamics of oil extraction from olive cake. Journal of American Oil Chemists' Society, 2008, 85(4), 391–396.

[62] Khan, N.U., Basal, H., Hassan, G. Cottonseed oil yield via economic heterosis and heritability in intraspecific cotton population. African Journal of Biotechnology, 2010, 9 (44), 7418–7428.

[63] Lawson, O.S., Oyewumi, A., Ologunagba, F.O., Ojomo, A.O. Evaluation of the parameters affecting the solvent extraction of soybean oil. ARPN Journal of Engineering and Applied Sciences, 2010, 5(10), 51–55.

[64] Ejikeme, P.M., Obasi, L.N., Egbuonu, A.C.C. Physico-chemical and toxicological studies on Afzelia Africana see and oil. African Journal of Biotechnology, 2010, 9(13), 1959 – 1963.

[65] Etong, D.I., Mustapha, A.O., Taleat, A.A. Physicochemical Properties and Fatty acid composition of Dikanut *(Irvingia Gabonensis)* seed oil. Research Journal of Chemical Sciences, 2014, 4(12), 70 – 74.

[66] Yusuf, O.S., Ezeja, M.I., Ugwudike, P.O. The physicochemical properties and fatty acid profile of oil extracted from *Irvingia gabonensis* seeds. International Journal of Biochemistry and Biotechnology, 2012, 2(2), 273 – 275.

[67] Ikya, J.K., Umenger, L.N., Lorbee, A. Effects of Extraction Methods on the Yield and Quality Characteristics of Oils from Shea Nut. Journal of Food Resource Science, 2013, 2(1), 1 – 12.

[68] Onoji, S.E., Iyuke, S.E., Igbafe, A.I. *Hevea brasiliensis* (Rubber Seed) Oil: Extraction, Characterization, and Kinetics of Thermo-oxidative Degradation Using Classical Chemical Methods. Energy and Fuel, 2016, 30(12), 10555–10567.

[69] Usman, M.A., Olanipekun, O.O., Henshaw, U.T. A Comparative Study of Soya Bean Oil and palm Kernel Oil as alternatives to Transformer oil. Journal of Emerging Trends in Engineering and Applied Sciences, 2012, 3(1), 33 – 37.

[70] Menkiti, M.C., Agu, C.M., Ejikeme, P.M., Onyelucheya, O.E. Chemically improved

Terminalia catappa L. oil: A possible renewable substitute for conventional mineral transformer oil. Journal of Environmental Chemical Engineering, 2017, 5, 1107–1118.

[71] Barbara, S. Analytical Techniques in Science. Infrared Spectroscopy; Fundamentals and Application: Wiley, 2004.